REPORT DOCUMENTATION PAGE

Form Approved
OMB No. 0704-0188

1. AGENCY USE ONLY (Leave blank)	2. REPORT DATE	3. REPORT TYPE AND DATES COVERED
	MAY 1995	FINAL - 1 DEC 92 TO 28 FEB 95

4. TITLE AND SUBTITLE
An Experimental Investigation of Cavity Acoustics in High Speed Flows

5. FUNDING NUMBERS
F49620-93-1-0079

6. AUTHOR(S)
Ahmad Vakili, Robert Wolfe, Paul Nagle

AFOSR-TR-95 0510

7. PERFORMING ORGANIZATION NAME(S) AND ADDRESS(ES)
University of Tennessee Space Institute
Tullahoma TN

9. SPONSORING / MONITORING AGENCY NAME(S) AND ADDRESS(ES)
Air Force Office Of Scientific Research
Aerospace & Materials Sciences Directorate
110 Duncan Avenue, Suite B-115
Bolling AFB DC 20332-0001

NA

10. SPONSORING / MONITORING AGENCY REPORT NUMBER
F49620-93-1-0079

11. SUPPLEMENTARY NOTES
ALSO APPENDIX A

12a. DISTRIBUTION / AVAILABILITY STATEMENT
APPROVED FOR PUBLIC RELEASE
DISTRIBUTION IS UNLIMITED

12b. DISTRIBUTION CODE

13. ABSTRACT *(Maximum 200 words)*

The research presented in this report has been directed to study the effects of mass injection into the flow upstream of a cavity to understand the weapon bay cavity's flow field and its aeroacoustics. The objective also was to control the development of upstream boundary layer, and therefore, to control the development of the shear layer over the cavity. Control of the shear layer has enabled us to significantly reduce or to fully eliminate the weapons bay's aeroacoustic interactions. This study was performed in a wind tunnel at several nominal Mach numbers between 0.5 to 1.8 and at unit Reynolds numbers up

14. SUBJECT TERMS	15. NUMBER OF PAGES
Cavity, Aero-acoustics	67
DTIC QUALITY INSPECTED 5	16. PRICE CODE

17. SECURITY CLASSIFICATION OF REPORT	18. SECURITY CLASSIFICATION OF THIS PAGE	19. SECURITY CLASSIFICATION OF ABSTRACT	20. LIMITATION OF ABSTRACT
U	U	U	U

An Experimental Investigation

of

Cavity Aeroacoustics in High Speed Flows

Final Report

for

Air Force Office of Scientific Research

(Grant F49620-93-1-0079)

by

Ahmad D. Vakili, Robert Wolfe

and

Paul A. Nagle

The University of Tennessee Space Institute

Tullahoma, Tennessee

May 1995

Table of Contents

SUMMARY

The research presented in this report has been directed to study the effects of mass injection into the flow upstream of a cavity to understand the weapon bay cavity's flow field and its aeroacoustics. The objective also was to control the development of upstream boundary layer, and therefore, to control the development of the shear layer over the cavity. Control of the shear layer has enabled us to significantly reduce or to fully eliminate the weapons bay's aeroacoustic interactions. This study was performed in a wind tunnel at several nominal Mach numbers between 0.5 to 1.8 and at unit Reynolds numbers up to 17 millions per foot. Measurements were performed for a number of injection distributions. The large amplitude oscillations measured without mass injection was successfully and totally eliminated with proper mass injection. Cavity oscillation amplitude has been reduced consistently by 27dB, for supersonic flows, from about 174dB (1.5psi) without mass injection to 147dB (0.07psi). In most cases the broad band noise level was also reduced appreciably. Measurements indicated that the upstream boundary layer and the shear layer characteristics over the cavity are significantly affected, altering the stability characteristics of the shear layer such that the feedback disturbances through the cavity could not match its instability frequency. Once the two frequencies are shifted apart there was no possibility for resonance interaction to take place leading to high amplitude peaks. For subsonic flows, a separate experimental study of mass injection effects on cavity aeroacoustics has been performed for Mach numbers of 0.5, 0.7 and 0.8. Mass injection rates of 0.05, 0.10, 0.15 and 0.2 lbm/s were used with three different mass injection patterns. Upstream mass injection led to the attenuation of cavity pressure oscillations between 12 and 17 dB. For a small range of Mach numbers between 0.68 and 0.72, frequency of the peak amplitude was observed to switch between modes 3 and 2, respectively. The measured frequencies were

in good agreement with predicted values calculated with the modified Rossiter's equation. Preliminary flow visualization studies in a water table show that mass injection may also attenuate the aeroacoustics in tandem cavity arrangements. The velocity profiles indicated that mass injection has changed the flow velocity profile downstream from the injection area. That mass injection produces most of its suppression effectiveness at low mass flow rates suggests either that the effect of boundary layer thickness on suppression is non-linear and or that other boundary layer parameters are of primary importance. The obvious candidates are the momentum thickness and or the $\frac{\partial^2 u}{\partial y^2}$ which determine the stability of the shear layer over the cavity. The upstream mass injection approach to control aeroacoustic interactions can be adapted to flow parameters inside and outside of the cavity to adjust the mass injection for active control of the cavity aeroacoustic levels with changing free stream. Combination of mechanical and upstream injection techniques may also be used and are being studied. Future efforts also focus on non-intrusive measurements over the injection area and on measuring velocity profiles at the various points. The upstream mass injection approach for control of aeroacoustic interactions can be adapted to flow parameters inside and outside of the cavity to adjust the mass injection for active control of the cavity aeroacoustic levels with changing free stream.

INTRODUCTION AND BACKGROUND

Cavity aeroacoustic oscillations are rapid, organized fluctuations in the pressure, density, and velocity of the fluid inside a cavity which has been exposed to flow over the open side of the cavity. Open cavity flow in shallow cavities is typically encountered in weapon bay applications. In this flow, the longitudinal pressure and flow oscillations have been associated to the shear layer interactions with the cavity.

Cavity oscillations have been observed to occur in wheel wells[1,2], ring cavities on projectiles[3,4], slotted wind tunnel walls[5,6], aerodynamic windows[7,8], bay vents on the Space Shuttle[9], and aircraft bomb bays[10]. The oscillations can cause structural deflection[11], structural fatigue[11], strong acoustic radiation[12], increased drag[13], and poor optical characteristics for aerodynamic windows[14]. The mechanism producing cavity oscillations consists of the interactions between the shear layer with the cavity. Shear layers are inherently unstable specially in the presence of acoustic perturbations which are resident within the cavity. Amplification and convection of the perturbations into the downstream results in interaction with the trailing edge and the production of upstream travelling influences[15]. The perturbation may manifest itself as resonant oscillation of the shear layer, vortex, or other vorticity fluctuation[16,17]. The perturbations are convected downstream and amplified as they convect. The amplification is selective and non-linear[35]. Upon reaching the trailing edge, the amplified perturbation interacts with the trailing edge and produces an upstream traveling influence. The upstream traveling influences are generally pressure disturbances, and may travel through the cavity, the shear layer, and the free stream (when subsonic). Remembering the instability of shear layers, the upstream traveling influence may create further shear layer perturbations, usually at or near the separations point[18]. When the upstream traveling influence and the downstream convecting perturbations are in proper phase, resonance may occur. The resonance may produce very high amplitude aeroacoustics inside the cavity.

Cavity oscillations are only occasionally considered desirable, therefore, researchers have usually sought to suppress them. Different approaches have been tried to reduce or eliminate the oscillations. Direct and indirect shear layer alteration includes passive venting of the cavity floor[19], mass injection through the cavity floor[20], and the presence of solid

objects inside the cavity, but touching the shear layer[21].

Separation and reattachment alteration includes leading and trailing edge structural modifications such as ramps[21]. Upstream boundary layer alteration includes cowls[17], vortex generators[22], spoilers[22], pin arrays[23], and upstream mass injection[24,25]. Combinations of the above approaches are also possible. However, almost all of these are passive techniques with relatively limited attenuation. And their effectiveness changes with the free stream flow parameters, sometimes resulting in worse than original conditions. The technique showing the greatest promise for the attenuation of cavity oscillations over a broad range of free stream mach numbers is upstream mass injection.

Mass may be injected parallel to the flow, transverse to the flow, or at any angle in between. The injection may take place through discrete holes, slots, screens, sintered surfaces, or other porous surfaces. The injection may be uniform or non-uniform over an area. Finally, the injection may be steady or unsteady. Uniform, steady, transverse injection is the focus of the present study.

Low rates of injection produce only modest effects on the boundary layer profile or the free stream flow[26]. Large rates of injection produce significant changes in the boundary layer velocity profile and the free stream[32]. Very large rates of injection may produce separation of the injected mass and the boundary layer[26]. The changes produced by mass injection also include the thickening of the boundary layer, increases in the momentum thickness and displacement thickness, and the formation of shocks when the free stream is supersonic[26,32].

In the current study, the primary purpose of boundary layer mass injection upstream

from a cavity is to alter the characteristics of the boundary layer. The shear layer over a cavity is formed from the separated upstream boundary layer, therefore, changes in the boundary layer could be expected to result in changes in the shear layer. When the changes in the shear layer interfere with or suppress the mechanism causing cavity oscillations, a reduction in the cavity oscillation amplitude is possible. The complexity of cavity flows and the lack of any comprehensive analytic model leads to the consideration of experimental or computational approaches.

The focus of this report is to present the results of several studies investigating the effectiveness of upstream mass injection in reducing cavity oscillations on the flow over shallow open cavities at subsonic to supersonic speeds.

REVIEW OF PREVIOUS

RELATED WORK

Krishnamurty[12], Roshko[13], Plumblee, Gibson, and Lassiter[31], Rossiter[17], Heller, Holmes, and Covert[28], Bilanin and Covert[29], Heller and Bliss[22], Sarohia[30], and Tam and Block[16] are a number of investigators who have attempted to understand cavity flows over the past four decades.

Computational cavity flow simulation has also been performed by many authors. Hankey and Shang[33] attempted a two dimensional simulation of the flow over a cavity with a L/D ratio of 2.25 and Mach number of 1.5. They solved the two dimensional Navier-Stokes equations using a time dependent, alternating direction explicit scheme by MacCormack. Turbulent closure was achieved by the Cebecci-Smith eddy viscosity model with relaxation modification. Their predictions of mean static pressures are reasonable compared to the experimental data of Heller and Bliss[37]. A spectral analysis of the results show reasonable agreement for the first and second cavity oscillation modes with respect to frequency and amplitude, also compared to data from Heller and Bliss[37], however, higher frequencies were not accurate.

Suhs[34] investigated a three dimensional cavity both with and without a leading edge spoiler. The cavity had a L/D ratio and L/W ratio of 4.5, flow Mach number was 1.2. He solved the Navier-Stokes equations using a thin layer approximation and an implicit solver using the Pulliam-Steger algorithm. Turbulence was modeled using the Baldwin-Lomax model. Both pressure distributions and frequency spectrums show good agreement with experimental data from Kaufman et al[38]. The spectrums were less accurate at higher frequencies and only predicted the first two modes of cavity oscillations. Both the cavity

with the spoiler and the cavity without the spoiler showed similar trends.

Suppression Studies

Suppression of cavity flow has also been widely studied. For example: Rossiter[17] noticed that the frequency spectrums differed significantly for two cavities of the same L/D ratio when one cavity was half the size of the other. He concluded that differing boundary layer thickness relative to cavity size was responsible. Rossiter then attached three solid spoilers to the leading edge of a cavity with a L/D ratio of 1 to see if the alteration of the flow over the cavity caused by the spoilers would suppress the pressure fluctuations. He was somewhat successful in reducing the oscillation amplitude, with the largest spoiler producing the greatest decrease.

Buell[8], Heller and Bliss[22], Franke and Carr[21] Smith, Gutmark, and Schadow[23] have studied various geometrical modifications and promising configurational changes to suppress the fluctuations, with limited success.

Sarno and Franke[31] investigated static and oscillating upstream boundary layer fences and steady and pulsating slot mass injection at the leading edge of a cavity with a L/D ratio of 2 and at Mach numbers from 0.6 to 1.5. The static fence was found to be most effective. However, it was only useful for suppressing the first resonance mode.

Sarohia and Massier[20] attempted to suppress the cavity oscillations occurring in a ring cavity at Mach numbers from 0 to 0.5 by steady injection of mass into the base of the cavity. They observed a reduction in pressure and velocity fluctuations as well as radiated sound. However, they also observed that the cavity oscillations were sometimes enhanced through slight unsteadiness in the mass injection.

Vakili and Gauthier[25] studied the suppression of cavity oscillations by upstream mass injection through plates with numerous holes at a Mach number of 1.8 and cavity L/D ratio of 2.54. They obtained almost complete suppression of the cavity oscillations. Broad band fluctuations were also reduced. The peak amplitudes produced by the cavity were reduced from 1.5 psi to 0.07 psi. They determined that at the lower mass injection rates, low area density injection produced greater suppression. They attribute the reduction in cavity oscillations to changes in the shear layer parameters and a resulting alteration in its instability characteristics.

EXPERIMENTAL PROCEDURE

The experimental effort was performed in the Gas Dynamics Laboratory at the University of Tennessee Space Institute. An 8 inch square subsonic/supersonic blowdown wind tunnel was used to produce a nominal free stream flow with Mach numbers from 0.5 to 1.8, and unit Reynolds numbers up to 17 million per foot. Static and dynamic pressures were measured and recorded digitally on line while the schlieren videos were taken.

Two different nozzles were used to establish the flow range noted above. A converging only nozzle was used for the subsonic regime, and a converging diverging nozzle block was used for the nominal Mach number of 1.8. A set of very interesting results were obtained when attempts were made to run the subsonic flow conditions with the supersonic nozzle block. These will be discussed later in the results section.

The tunnel floor is employed to simulate the fuselage of an aircraft onto which the weapon bay cavity is installed. This arrangement allows an increase in model size, adds to flexibility of the simulation, allows for desirable thickness of the boundary layer (shear layer) over the cavity, and accommodates simplicity in measurements. The rectangular cavity had internal dimensions of 1.5 inches wide by 1.5 inches deep by 6.5 inches long, representing an L/D of 4.33, which is somewhat similar to flight hardware. Other cavities with L/D of 2.0 and 2.54 has also been studied previously, with similar results observed. The cavity model was constructed of aluminum and inset flush into the floor of the tunnel test section about 4 inches downstream of the nozzle exit.

The bottom of the cavity contained one static pressure port, two access ports for dynamic pressure transducers, and one access port for the traversing probe. Dynamic

pressure transducers were flush mounted for optimum response. The access ports were sealed when any of the probes were not in use. Figure 1 illustrates the experimental setup with the cavity and the instrumentation used shown on Figure 2.

Mass was injected through perforated plates, 2.0 inches wide by varying length, number of holes, size of holes, and distribution of holes. The injection plates were located immediately upstream of the cavity and constructed from aluminum. The injection plate was supplied with air from a plenum located beneath, and the plenum was supplied by a two inch pipe from high pressure air tanks. An orifice plate and two static ports were installed in the supply pipe to measure the mass flow rate. Figure 3 shows the overall injection distribution for five selected injection plates. Plate 1 is identified as high density injection. Plate 2 had 90 holes with diameters of .0625 inches, plate 4 is the same as plate 2 except that the holes have a diameter of 0.03125 inches. Plate 9 had 190 holes with diameters of .03125 inches, the holes for Plate 9 were distributed in three streamwise rows, and plate 8 had 350 holes with diameters of .015625 inches.

Two five hole cone probes, one with a 15° half angle and one with a 30° half angle, were used in a traversing mechanism. The probes were used to determine flow angularity as well as Mach number. However for the present effort the central port was used to measure the total pressure and flow speed was calculated. The probes were 0.070 inches in diameter and the five ports were 0.008 inches in diameter. The probes were mounted in holders which could be traversed vertically during the tunnel runs. The probes were installed at two streamwise positions inside the tunnel. At forward position where the probe tip was just at the cavity leading edge and at downstream position where the probe tip was just at the cavity trailing edge. One holder had a rotatable crank arm allowing it to reach two

stations at both the front and back positions. The holders were moved by a threaded shaft connected to a stepper motor. The stepper motor was controlled during tunnel runs by a computer. The probes were traversed at six stations near the cavity, shown in Figure 4.

The test section of the tunnel, where the cavity was installed, was 48 inches long. The injection plate and cavity are preceded by one static port on the floor center line. Tunnel sides walls and the ceiling of the test section adjacent to the injection plate and cavity are transparent and allow Schlieren videotape to be taken. The transparent sections do not extend into the cavity. Therefore, no images from within the cavity could be recorded. There are also static pressure ports on each side of the cavity. Downstream of the cavity is another access port for the traversing probe to allow shear flow measurements at the downstream of the cavity. Downstream of the access port, on the tunnel center line, are twenty four static ports located on one inch centers. Figure 5 illustrates the various ports and their locations.

The static ports in the downstream were connected to a Scanivalve using a Scanivalve PDCR24 transducer. All other static ports were connected to Validyne DP15 transducers. The dynamic pressure transducers are Endevco models 8514-10 and 8510-c-15. The Validyne transducers were connected to Validyne CD19 amplifiers. The Endevco transducers used Validyne SG71 amplifiers. The amplifier outputs were connected to an analog-to-digital converter attached to a Northgate 286 IBM compatible personal computer.

The amplified dynamic pressure transducer signals were also connected to two spectrum analyzers. Each signal was routed to an HP3582A Spectrum Analyzer as well as to a 486 personal computer running Labview software. The spectrum analyzers averaged either 8 or 16 sets of data, each set containing 1024 data points collected at 10,000 data points per second.

Tunnel runs, probe movement, and data acquisition were controlled using programs run on the Northgate 286 personal computer. Both probe data and spectrum data could not be collected during the same tunnel run.

The procedures used in collecting data were generally similar for both the collection of dynamic pressure data and the cone probe traverses. All runs start by zeroing the transducer amplifiers and adjusting the schlieren when it was used. The tunnel was started by an operator, and the nominal flow Mach number was established. When dynamic pressure data was measured, the spectrum analyzers were triggered by one person at a signal from the tunnel operator who also triggered the data collection program and controlled the mass injection rate. When the cone probe was traversed the tunnel operator triggered a different data collection program which also controlled the probe traversing mechanism. A second person was generally used to control the mass injection rate during probe traverse runs. The probe traverses were slowed by the need to park the probe at each point for over a second to allow the pressure inside of the probe system to come to equilibrium. The parking time was required due to the very small diameter of the flow passages inside the cone probe and the relatively long length of the connecting tubing.

RESULTS AND DISCUSSIONS

The results of the experimental effort may be divided into two areas: subsonic and supersonic observations. Each of these areas may be further divided into two sub areas. The first sub area involves dynamic pressure spectrum data for several injection plates at different mass injection rates. Only the most physically relevant information have been discussed here, while the remainder of data collected are presented in the Appendices in graphic or tabulated format. The second sub area includes flow field measurements with cone probes to determine velocity profiles for selected plates with different mass injection rates.

For the subsonic flow regimes, dynamic frequency spectra was recorded for the cavity with and without upstream mass injection at Mach numbers of 0.5, 0.7 and 0.8. Figures 6 a and b are the frequency spectra for channel 0 and channel 1 at Mach number 0.5. Channel 0 depicts the dynamic pressure transducer near the downstream wall of the cavity, channel 1 is output from the dynamic transducer near the leading edge of the cavity. Figure 6a shows the baseline (cavity without mass injection) pressure spectra and shows a peak amplitude for both channels occurring at a frequency of 1320 Hz with a magnitude of -14.99 dBv, for channel 0. This correspond to 156dB, where: dB = 20 log(P/Pref), Pref= 2 x 10^{-5} N/m^2. Figure 6b is a similar frequency spectra taken with 0.10 lbm/sec upstream mass injection (blowing parameter B=1.2) for plate 9. Comparing 6a and 6b we see that the result of mass injection is the total reduction of the peak amplitudes in both channels. An observation which is not readily noticeable is the slight increase in broad band noise energy with mass injection for frequencies greater than about 2000 Hz. This suggests that some energy is dispersed to the higher frequencies. No explanation of how or why this has occurred has been determined; the effect, however, is not a major concern. Results are similar for plates

2 and 4 with a reduction of the peak amplitude and an increase in broad band energy above the frequency of approximately 2000 Hz. At a low mass injection rate of 0.05 lbm/s the large peak was reduced but not as much as at higher rates for plates 2 and 4. Plate 9 had the greatest effect of suppressing cavity aeroacoustics at Mach 0.5. Compared to all three plates, mass injection through plate 9 was able to reduce completely the peak amplitude at all mass injection rates. The reduction was possibly due to a different streamwise vorticity pattern generated by the injection through plate 9, which helped to better control the shear layer.

Figures 7 a, b and c are frequency spectra responses for Mach 0.7. An interesting phenomena of frequency switching occurred for the baseline measurements for a small Mach number range around 0.7. Figure 7a is the baseline representative spectra for the Mach number range of 0.68 to 0.7. Here two peaks are distinguishable with the peak at 1660 Hz being the most prominent. Figure 7b is a baseline frequency spectrum representative for the Mach number range of 0.7 to 0.72. The peak frequency is now switched to 1084 Hz which was previously the weak peak on figure 9a and the peak amplitude at 1660 Hz is significantly reduced. It is believed that this switching of mode frequencies are similar to the observations of Rossiter[2]. At a Mach number of 0.7 for a cavity L/D ratio of 2, Rossiter noticed that there seemed to be no real dominant frequency. Figure 9c is the response with 0.10 lbm/s mass injection from plate 9, and again the peak amplitudes have been reduced. Similar results were obtained for different plates and mass injection amounts. Plate 9 was most effective at the low mass injection rates while plate 2 was most effective at the higher flow rates.

Figures 8 a, b, c and d present frequency spectra for Mach 0.80. Figure 8a is the

baseline spectra and shows the peak frequency to be at 1113 Hz, with minor peaks at frequencies of about 500 Hz and 1800 Hz. Unlike the responses for plates 2 and 4 at the other Mach numbers, the effect of mass injection at Mach 0.80 was different. Figure 8b shows that at a low mass injection rate of 0.05 lbm/s through plate 2, the peak amplitude actually increases. As the mass injection rate was increased to 0.15 lbm/s and higher the peak amplitudes began to be reduced. Figure 8c shows the spectra for Mach 0.80 at a mass injection rate of 0.15 lbm/s using plate 2. Higher mass rates were not obtainable. The larger plenum pressures needed, for the higher mass flow rates, blew out seals around the mass injection apparatus. The result gave false readings about the amount of mass actually involved in changing the boundary layer structure in the tunnel. Figure 8d shows the results of the frequency spectra for plate 9 at 0.05 lbm/s. Plate 9 was the exception in that at the low mass injection rate of 0.05 the peak amplitude was reduced, but at higher injection rates the response was again an increase in peak amplitude.

Figure 9 is a plot showing the baseline peak amplitude frequency for each Mach number compared to the empirical values of frequency given by the modified Rossiter's equation,

$$St = f\frac{U}{L} = \frac{m - n}{\frac{M}{\sqrt{1+\frac{\gamma-1}{2}m^2}} + \frac{1}{k_v}} \cdot$$

Here St is the Strouhal number, m is the mode (m = 1,2 3, ...), Kv is the ratio of convected vortex velocity to free stream velocity and n is the acoustic wave emission delay constant. Kv and n are empirically derived and are equal to 0.57 and 0.25, respectively, for an L/D ratio of 4. The present experimental results are in good agreement with the empirical equation, with only a 3 percent difference. However, compared with the experimental data of Rossiter[2] at each Mach number the frequency mode numbers corresponding to aeroacoustical peak frequencies did not coincide. Dissimilarities in frequency mode numbers were attributed to

the difference between Rossiter's cavity (L/D=4) and the cavity in this study (L/D=4.33). The mode value is not predictable and depends upon the cavity and flow conditions.

Figures 10 and 11 are Schlieren photographs taken from a VCR camera and frame grabbed using a Data Translations frame grabbing board installed in a 486 PC. Figure 10 shows the boundary and shear layer over the cavity at a Mach number of 0.7. There is no mass injection present upstream. The first vertical line from the right would be the start of the mass injection area. The second vertical line is the location of the leading edge of the cavity. The third vertical line just visible in the left corner of the photograph is the location of the cavity's trailing edge. The four horizontal marking dashes just downstream of the second vertical line are approximately 0.25 inches apart with the bottom line the same distance from the floor of the tunnel. It is observed that the boundary layer is approximately 0.2 to 0.3 inches thick. The ratio of the boundary layer thickness to cavity length and depth are $\frac{\delta}{L} = 0.046$ and $\frac{\delta}{D} = 0.2$, respectively. Figure 11 is a similar photograph to that of figure 12 except with mass injection present. It shows the effect of a mass injection rate of 0.10 lbm/s from plate 4 on a Mach 0.7 free stream flow. The shear layer is thickened over the cavity so that it does not interact with the cavity or the trailing edge. The boundary layer thickness to Length and Depth ratios are estimated to be about twice as large as with no mass injection.

Figures 12, 13 and 14 are plots of sound pressure level reduction versus mass injection rate for the various Mach numbers. The greatest amount of reduction shown in figure 13 is for a Mach number of 0.7 with a mass injection of 0.1 lbm/s, using plate 2. The greatest reduction for all plates occurs around 0.1 lbm/s of mass injection for Mach numbers of 0.5 and 0.7. Figure 14 shows that at Mach 0.8 the greatest reduction of sound pressure

level occurs at higher mass injection rates, with an increases in peak amplitude occurred at 0.05 lbm/s mass injection. Figure 14, plate 9 shows a range of mass injection where there is reduction in peak amplitude around the mass injection rate of 0.05 lbm/s. The magnitude of reduction decreases and then again increases at 0.2 lbm/s. One of the possible explanations for this is transonic effects. These test conditions were repeated several times to assure that there was not any problems with the measuring instruments. Each measurement was consistent with the previous measurement, which was a measure of repeatability of the data gathered. Figure 15 through 17 are similar plots of peak amplitude reduction in acoustic sound pressure levels versus the blowing parameter B*(Ainj/Apattern) for plates 2, 4 and 9.

Table I is a summary of the maximum reduction of cavity oscillations for each plate, Mach number, and mass injection rate tested. Observations of the blowing parameter show ranges where injection was most effective. The effective range of the blowing parameter for the Mach number of 0.5 was around 0.1 to 0.2 and for the Mach number of 0.7 the range was 0.06 and 0.07, for all mass injection plates. An effective range of the blowing parameter for the Mach number of 0.8 was not as distinct. The level of blowing seemed to be dependent upon the distribution of the injection pattern. As previously stated, for a Mach number of 0.8 higher mass injection rates worked well with plates 2 and 4, and for plate 9 lower injection rates between 0.05 to 0.06 lbm/s were more effective.

Table II contains typical selected results for a few plates at supersonic flow. The table contains the peak amplitude at the downstream dynamic pressure transducer port in pounds per square inch (psi), and sound pressure level (dB). The table also contains the blowing parameter $B = \frac{\rho_w U_w}{\rho_\infty U_\infty}$, and two derived parameters, $B_c = \frac{\rho_w U_w A_{inj}}{\rho_\infty U_\infty A_{cav}}$, which equals B

multiplied by the ratio of the injection area to the cavity floor area, and $B_d = \frac{\rho_w U_w A_{inj}}{\rho_\infty U_\infty A_{injdis}}$, which equals B multiplied by the ratio of the injection area to the area contained within the perimeter of a rectangle which just circumscribes all the injection holes. The blowing parameter is more appropriate to uniform injection over a surface. In the present situation, injection is taking place over a small region of the flow. The authors feel more comfortable with B_c or B_d as a measure of non-dimensional mass injection in this case. The almost complete suppression of the peak pressure oscillations as well as a reduction in the broad band fluctuations is apparent from the table and the figures.

Figure 18 presents the amplitude reduction, for supersonic flow, resulting from mass injection versus the mass injection rate for various plates. The no mass injection amplitudes are used as the reference. The error bars are ±2 dBV and were observed during 12 consecutive runs without mass injection. Data on this figure demonstrates the diminishing returns for mass injection above 0.05 lbm/s. Plate 8 appears to suppress the cavity oscillations best. Figure 19 graphs the amplitude reduction versus the injection area of selected plates at three mass injection rates. Lower injection areas provide improvement in amplitude reduction, although when the injection area is zero the reduction must also be zero. Subsonic data are also shown for reference on these figures.

Figures 20 through 25 are velocity profiles derived from pressure data collected by the cone probe traverses. The data was collected for supersonic flow at six stations and three mass injection rates with injection through plate 8. The profiles from stations D and E (as shown in figure 4) had to be truncated and the highest mass injection rate for station D is absent. The highest injection rate data for station D could not be reduced. The data for stations D and E showed that some lower profile points had probe total pressures

lower than the free stream static pressures and these points are not shown. A possible explanation for this might be entrainment of the boundary layer by the discrete jets and/or off angle flow approaching the probe. The profiles show significant changes as mass injection is increased, with the changes largely restricted to the region directly behind the injection plate. Inflections points in the profiles appear and move upward as the mass injection rate increases. The boundary layer thickness also increases but this is less pronounced than the profile changes.

Considering the linear stability theory, Reshotko[39], the stability of a boundary layer (shear flow) decreases as its second derivative near the wall becomes more positive. The two dimensional boundary layer equation near the wall may be written as:

$$\mu_w \frac{\partial^2 u}{\partial y^2} = \left(\rho v_w - \frac{d\mu}{dT}\frac{\partial T}{\partial y}\right)\frac{\partial u}{\partial y} + \frac{dp}{dx}$$

Any of the three terms on the right hand side of the above equation affect the second derivative on the left. For the present case, in the absence of heat transfer, the mass injection and the resulting pressure gradient clearly change the stability of the boundary layer. This in turn changes the stability characteristics of the shear layer over the cavity. Measurements indicated that the upstream boundary layer and the shear layer profiles over the cavity are significantly affected, altering the stability characteristics of the shear layer. The changes are such that the feedback disturbances through the cavity could not match its roll up frequency. Once the two frequencies are shifted apart, there can be no possibility for resonance interaction to take place leading to high amplitude oscillations.

The upstream mass injection approach to control aeroacoustic interactions can be adapted to flow parameters inside and outside of the cavity to adjust the mass injection for active control of the cavity aeroacoustic levels with changing free stream.

An interesting observation was made when we tried to operate the tunnel in the subsonic mode with the supersonic nozzle installed. With all other arrangements remaining the same, the tunnel was operated off design with a normal shock in the nozzle resulting in a Mach 0.5 free stream flow. This resulted in a quite thick boundary layer (one inch, compared to the 0.375 inches) just upstream of the cavity. Pressure measurements inside the cavity did not reflect the large amplitude aeroacoustic oscillations expected in the cavity. Detail of this study is presented by Lambert[36]. Similar measurements with a converging only nozzle, resulting in a thin boundary layer at the cavity, resulted in distinct pressure peaks.

Depending on the free stream flow conditions the effectiveness of an injection pattern for a given mass flow rate was found to be different. This is evidenced from a large number of runs made and are outside of the scope of this paper to be discussed in detail. The information presented here supports the trend and the above conclusion.

From the above observations it is clear that the stability characteristic of the shear layer over the cavity is critical to the generation of the high amplitude peaks. Depending on the free stream flow parameters, shear layer over the cavity changes, resulting in different instabilities. This also explains the lack of uniform effectiveness for various passive control techniques. The mass injection rate as well as the injection pattern and area may be readily adapted to the free stream changes. This enables one to actively control the aeroacoustics in a cavity, over a wide range.

It is also possible to combine mechanical devices with the upstream injection to accomplish the same results. This aspect is the subject of a separate investigation and will be reported elsewhere.

Cone Probe Measurements in the Wind Tunnel

Figures 26 through 29 are vector plots of velocity in the shear layer over the cavity. As shown in figure 4, only three station over the cavity could be measured each at both the leading and trailing edge of the cavity. The cone probe support device did not allow any other positions to be measured. To obtain a better understanding of the flow over the cavity, the mirror image of the data measured at stations 1, 2, 4 and 5 was incorporated into plot. The scale vector is equal to a Mach number of 0.25. Like Wolfe[40] the static pressure measurements of the cone probe were influenced by the mass injection process and at times were greater than the local total pressure measurement. Some sections of the data were not reducible and gaps can be seen on the plot.

Figures 26 and 27 are surveys of the shear layer at the leading and trailing edge respectively for a Mach number of 0.7 with no mass injection present. The center line traversing survey, in figure 26, shows that a very small amount of cross flow was measured. Theoretically this cross flow should not exist because of the assumption that the tunnel flow has a mid-plane symmetry. The probe may not have been exactly lined up with the center line of the tunnel flow, or the cavity giving measurements off the plane of symmetry. Figure 27 shows that a small amount of rotation is in the flow near the trailing edge possibly due to flow entrainment caused by the unsteady nature of the shear layer.

Figures 28 and 29 are vector plots at the same Mach number as figures 26 and 27, but with a mass injection rate, through plate 4, of 0.1 lbm/s. Figure 28 displays the measurements at the upstream location, and shows streamwise, rotational structures starting to develop above the cavity. These structures occur at approximately 0.5 inches above the floor of the tunnel. Although, there are no measurements to indicate such, the height that

the vortex structures are observed in figure 28, seem to coincide with the point were the probe left the injection wedge as shown in figure 11. Vakili et al[21] had previously suggested the existence of the streamwise vortices and their relative positions above the cavity. Their suggestion was based upon the results of their study, which evaluated the effectiveness of several mass injection distributions to reduce cavity aeroacoustic oscillations .

Water Table Experiments

Figure 30 and 31 are video images photographed from the water table and then image grabbed using the technique previously described. They show the effects of mass injection on both a single and double cavity arrangement. The flow conditions represent a Froude number of 2.16. Figure 30 dramatically shows the effects of mass injection on a single cavity. In figure 30a, the wave pattern is reflecting downward into the cavity and later bounces off the floor and interacts with the shear layer near the trailing edge, something that Tam and Block[3] said could be a significant influence. Figure 30b shows how a mass injection rate of 4 gallons/min (0.56 lbm/s) affects the cavity flow. The flow is much smoother and much less chaotic. For a single cavity, with suction at the trailing edge, the pressure oscillations were still prevalent in the cavity.

Figure 31 shows how mass injection influences a double cavity arrangement. Close observations of figure 31a show that the leading cavity is perturbed, while the second cavity's pressure oscillations are not as severe. At higher mass injection rates figure 31b shows that both cavities seem to be less unsteady . Qualitatively this indicates that mass injection may also be sufficient to reduce cavity pressure oscillations in both single and double in-line cavity arrangements.

Computational Effort

A systematic effort was undertaken to calculate the flow field of the experimental set-up to help guide the direction of the experiments and also to develop a possible amplitude prediction tool. The effort was not successful and is not reported here. A complete description of the computational approach and results are given in the Master Thesis of Wolfe[40].

CONCLUSIONS AND REMARKS

The effectiveness of upstream mass injection in suppressing cavity oscillations is related to the amount of mass injected and the distribution of the injection. The greatest incremental improvements in suppression effectiveness takes place at a nominally low flow rate. For higher mass flow rates suppression effectiveness is actually reduced. Upstream mass injection can be used to successfully eliminate large amplitude aeroacoustic peaks observed in cavities. This also resulted in a large reduction in the broad band amplitudes. The flow field resulting from the upstream mass injection demonstrates a reduction in the energy contained in the shear layer fluctuations, not a redistribution of the energy within the pressure spectrum. Cavity oscillation amplitude has been reduced consistently by up to about 27dB, for supersonic flow of a nominal Mach number of 1.8, from about 174dB (1.5psi) without mass injection to 147dB (0.07psi). Large attenuation in the peak amplitudes were obtained for subsonic flows.

All of the supersonic measurements were performed at a nominal Mach number of 1.8. For subsonic flows, a separate experimental study of mass injection effects on cavity aeroacoustics has been performed of Mach numbers of 0.5, 0.7 and 0.8. Mass injection rates of 0.05, 0.10, 0.15 and 0.2 lbm/s were used with three different mass injection patterns. The following conclusions have been drawn:

With a sufficient amount of upstream mass injection the attenuation of cavity pressure oscillations were between 12 and 17 dB.

For a small range of Mach number between 0.68 and 0.72, frequency of the peak amplitude was observed to switch between modes 3 and 2, respectively. The measured

frequencies were in good agreement with predicted values calculated with the modified Rossiter's equation.

Cone probe measurements indicate the presence of streamwise vortices, which may play a strong role in controlling the unsteadiness of the shear layer and reducing cavity pressure oscillations.

The mass injection pattern of distribution played a critical role at Mach number 0.8 in amplitude reduction of pressure oscillations. This may be related to transonic effects and to differences in the way the streamwise vortices and transverse vortices interact with each other at the higher flow speeds.

Preliminary flow visualization studies in a water table show that mass injection may also attenuate the aeroacoustics in a double in-line cavity arrangement. Also, suction at the trailing edge of the cavity was appears to be much less effective in reducing cavity pressure oscillations.

The velocity profiles indicated that mass injection has changed the flow velocity profile downstream from the injection area. The profiles seem to indicate that boundary layer thickness is most affected at higher mass flow rates. That mass injection produces most of its suppression effectiveness at low mass flow rates suggests either that the effect of boundary layer thickness on suppression is non-linear and or that other boundary layer parameters are of primary importance. The obvious candidates are the momentum thickness and or the $\frac{\partial^2 u}{\partial y^2}$ which determine the stability of the shear layer over the cavity, as discussed earlier. This supports the earlier work of Vakili et al.[25] who had theorized that injection changes the stability of the shear layer through changes in the separating boundary layer and its

derivative parameters.

The upstream mass injection approach to control aeroacoustic interactions can be adapted to flow parameters inside and outside of the cavity to adjust the mass injection for active control of the cavity aeroacoustic levels with changing free stream. Combination of mechanical and upstream injection techniques may also be used and are being studied. Future efforts also focus on non-intrusive measurements over the injection area and on measuring velocity profiles at the various points.

It is recommended to continue this study to develop a theoretical understanding for the mechanisms involved in determination of the oscillation amplitude.

REFERENCES

[1] Gibson, J.S., "Non Engine Aerodynamic Noise Investigation of a Large Aircraft", NASA CR 2378, October 1973.

[2] Bliss, D.B. and Hayden, R.E., "Landing Gear and Cavity Noise Prediction", NASA CR 2714, July 1976.

[3] Parthasarathy, S.P., Cho, Y.I., and Back, L.H., "Aerodynamic Sound Generation Induced By Flow Over Small Cylindrical Cavities", AIAA Paper No. 84-2258, October 1984.

[4] Parthasarathy, S.P., Cho, Y.I., and Back, L.H., "High Intensity Tone Generation by Axisymmetric Ring Cavities on Training Projectiles", AIAA Paper No. 84-2259, October 1984.

[5] Mabey, D.G., "Resonance Frequencies of Ventilated Wind Tunnels", AIAA Journal, Vol.18, No.1, January 1980, pp. 7-8.

[6] Bliss, D.B., "Aerodynamic Behavior of a Slender Slot in a Wind Tunnel Wall", AIAA Journal, Vol.20, No.9, September 1982, pp. 1244-1252.

[7] Shen, P., "Supersonic Flow over a Deep Cavity for a Laser Application", AIAA Journal, Vol.17, No.2, February 1979, pp.216-219.

[8] Buell, D.A., "An Experimental Investigation of the Airflow Over a Cavity with Antiresonance Devices", NASA TN D-6205, 1971.

[9] Tanner, C.S., "Shuttle Cargo Bay Vent Noise and its effects on Generic Payload Specifications and Testing Methods", AIAA Paper No. 84-2352, October 1984.

[10] Norton, D.A., "Investigation of B47 Bomb Bay Buffet", Boeing Airplane Company, Document No. D12675, May 1952.

[11] Goldman, R.L., Morkovin, M.V., and Schumacher, R.N., "Unsteady Control Surface

Loads of Lifting Reentry Vehicles at Very High Speeds", AIAA Journal, Vol.6, No.1, January 1968, pp.44-50.

[12] Krishnamurty, K., "Acoustic Radiation from Two- Dimensional Rectangular Cutouts in Aerodynamic Surfaces", NACA TN 3487, August 1955.

[13] Roshko, A., "Some Measurements of Flow in a Rectangular Cutout", NACA TN 3488, August 1955.

[14] Avidor, J.M., "Improved Free Vortex, Subsonic Aerodynamic Window", AIAA Journal, Vol.17, No.2, November 1979, pp.216-219.

[15] Rockwell, D., "Oscillation of Impinging Shear Layers", AIAA Journal, Vol.21, No.5, May 1983, pp.645-664.

[16] Tam, C.K.W., and Block, P.J.W., "On the Tones and Pressure Oscillations Induced by Flow Over Rectangular Cavities", Journal of Fluid Mechanics, Vol.89, Part 2, 1978, pp.373-399.

[17] Rossiter, J.E., "Wind Tunnel Experiments on the Flow Over Rectangular Cavities at Subsonic and Transonic Speeds", ARC R&M No.3438, October 1964.

[18] Komerath, N.M., Ahuja, K.K., and Chambers, F.W., "Prediction and Measurement of Flows Over Cavities- A Survey", AIAA Paper No. 87-0166, January 1987.

[19] Wilcox, F.J.Jr, "Passive Venting System for Modifying Cavity Flow Fields at Supersonic Speeds", AIAA Journal, Vol.26, No.3, March 1988, pp.374-376.

[20] Sarohia, V., and Massier, P.F., "Control of Cavity Noise", AIAA Journal of Aircraft, Vol.14, No.9, September 1977, pp.833-837.

[21] Franke, M.E., and Carr, D.L., "Effect of Geometry on Open Cavity Flow Induced Pressure Oscillations", AIAA Paper No. 75-492, March 1975.

[22] Heller, H.H., and Bliss, D.B., "The Physical Mechanism of Flow Induced Pressure

Fluctuations in Cavities and Concepts for their Suppression", AIAA Paper No. 75-491, March 1975.

[23] Smith, R.A., Gutmark, E., and Schadow, K.C., "Mitigation of Pressure Oscillations Induced by Supersonic Flow Over Slender Cavities", AIAA Paper No. 90-4019, October 1990.

[24] Vakili, A.D., Wu,J.M., and Taylor, M., "Shear Flow Control Applied to Suppress Cavity Oscillations and Improve Store Separation", Weapons Carriage and Separation Workshop, Wright Patterson AFB, Dayton OH,April 1988.

[25] Vakili, A.D., and Gauthier, C., "Control of Cavity Flow by Upstream Mass Injection", AIAA Journal of Aircraft, Vol.31, No.4, January-February 1994, pp.169-174.

[26] Fernandez, F.L., and Zukoski, E.E., "Experiments in Supersonic Turbulent Flow with Large Distributed Surface Injection", AIAA Journal, Vol.7, No.9, September 1969, pp.1759-1767.

[27] Plumblee, H.E., Gibson, J.S., and Lassiter, L.W., "A Theoretical and Experimental Investigation of the Acoustic Response of Cavities in an Aerodynamic Flow", WADD-TR-16-75, March 1962.

[28] Heller, H.H., Holmes, D.G., and Covert, E.E., "Flow Induced Pressure Oscillations in Shallow Cavities", Journal of Sound and Vibration, Vol.18, No.4, 1971, pp.545-553.

[29] Bilanin, A.J., and Covert, E.E., "Estimation of Possible Excitation Frequencies for Shallow Rectangular Cavities", AIAA Journal, Vol.11, No.3, March 1973, pp 347-351.

[30] Sarohia, V., "Experimental Investigation of Oscillations in Flows Over Shallow Cavities", AIAA Journal, Vol.15, No.7, July 1977, pp.984-991.

[31] Sarno, R.L., and Franke, M.E., "Suppression of Flow Induced Pressure Oscillations in Cavities", Journal of Aircraft, Vol.31, No.1, January-February 1994, pp.90-96.

[32] Goldstein, R.J., Shavit, G., and Chen, T.S., "Film- Cooling Effectiveness with Injection through a Porous Section", ASME Journal of Heat Transfer, August 1965, pp.353-361.

[33] Hankey, W.L., and Shang, J.S., "Analysis of Pressure Oscillations in an Open Cavity", AIAA Journal, Vol.18, No.8, August 1980, pp.892-898.

[34] Suhs, N.E., "Unsteady Flow Computations for a Three- Dimensional Cavity with and without an Acoustic Suppression Device", AIAA Paper No. 93-3402, August 1993.

[35] Ho, C.M., and Huerre, P., "Perturbed Free Shear Layers", Annual Review of Fluid Mechanics, Vol.16, 1984, pp.365- 424.

[36] Lambert, E.P., "Measurements of the Shear Layer Over a Cavity with and without Upstream Mass Injection", Masters thesis, University of Tennessee-Knoxville, August 1994.

[37] Heller, H., and Bliss, D., "Aerodynamically Induced Pressure Oscillations: Physical Mechanisms and Suppression Concepts", Wright-Patterson Air Force Base, Ohio, AFFDL-TR-74-133, February 1975.

[38] Kaufman, L.G.II, Maciulaitis, A., and Clark, R.L., "Mach 0.6 to 3.0 Flows Over Rectangular Cavities", AFWAL-TR- 82-3112, May 1883.

[39] Reshotko, E.," Stability and Transition, How Much Do We Know?," ASME, New York, 1987, pp. 412-434

[40] Wolfe, R.C.," An Investigation of the Effects of Upstream Mass Injection on Cavity Oscillations", The University of Tennessee, May, 1995.

FIGURES

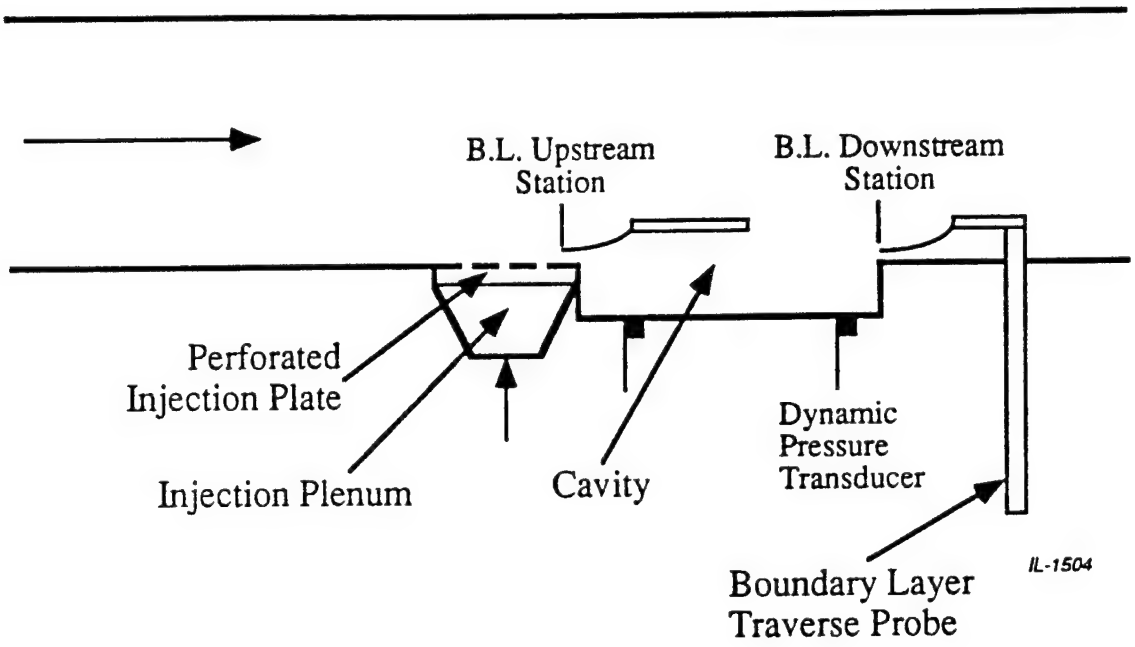

Figure 1. Schematic of the experimental setup.

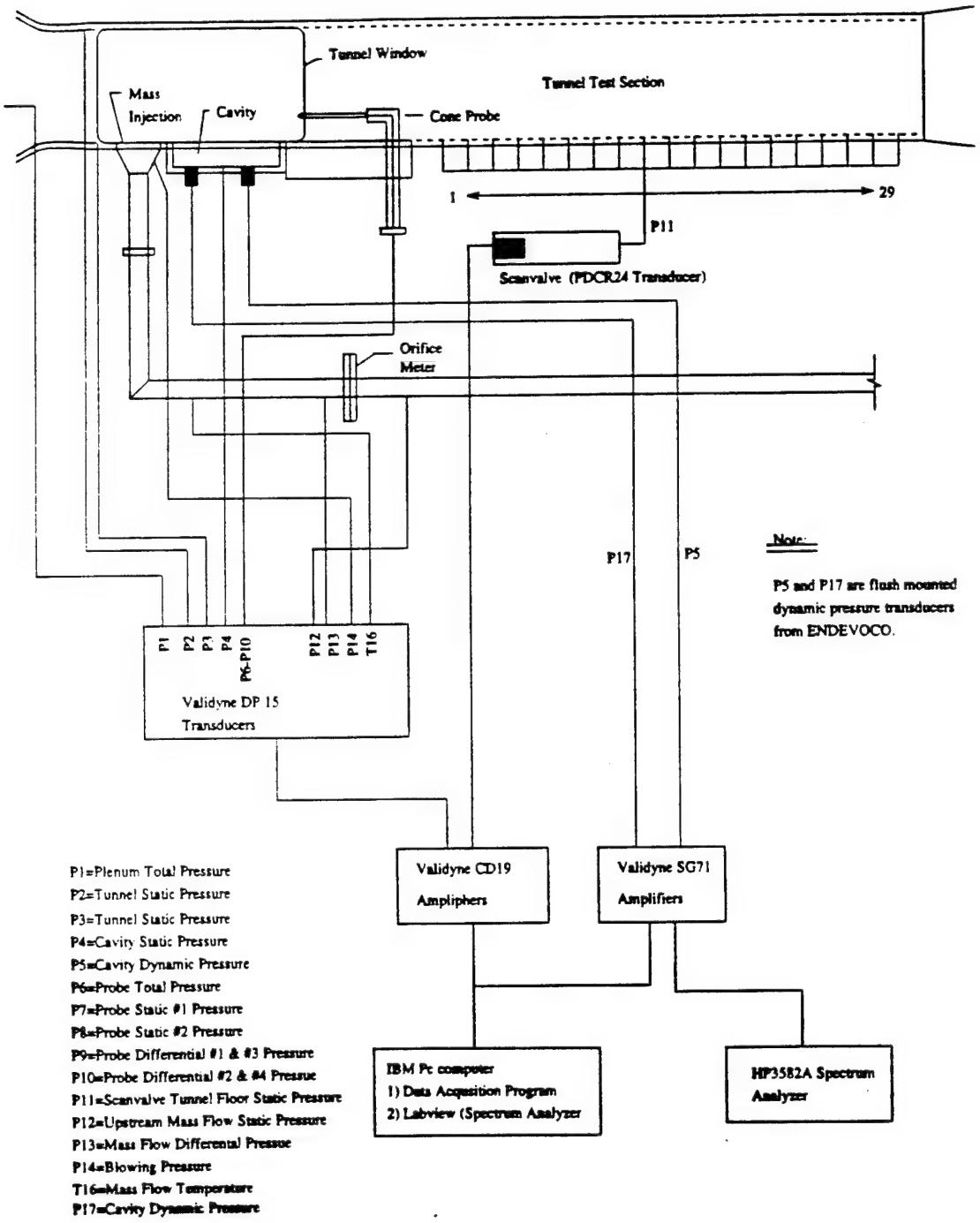

Figure 2. Schematic of the experimental setup.

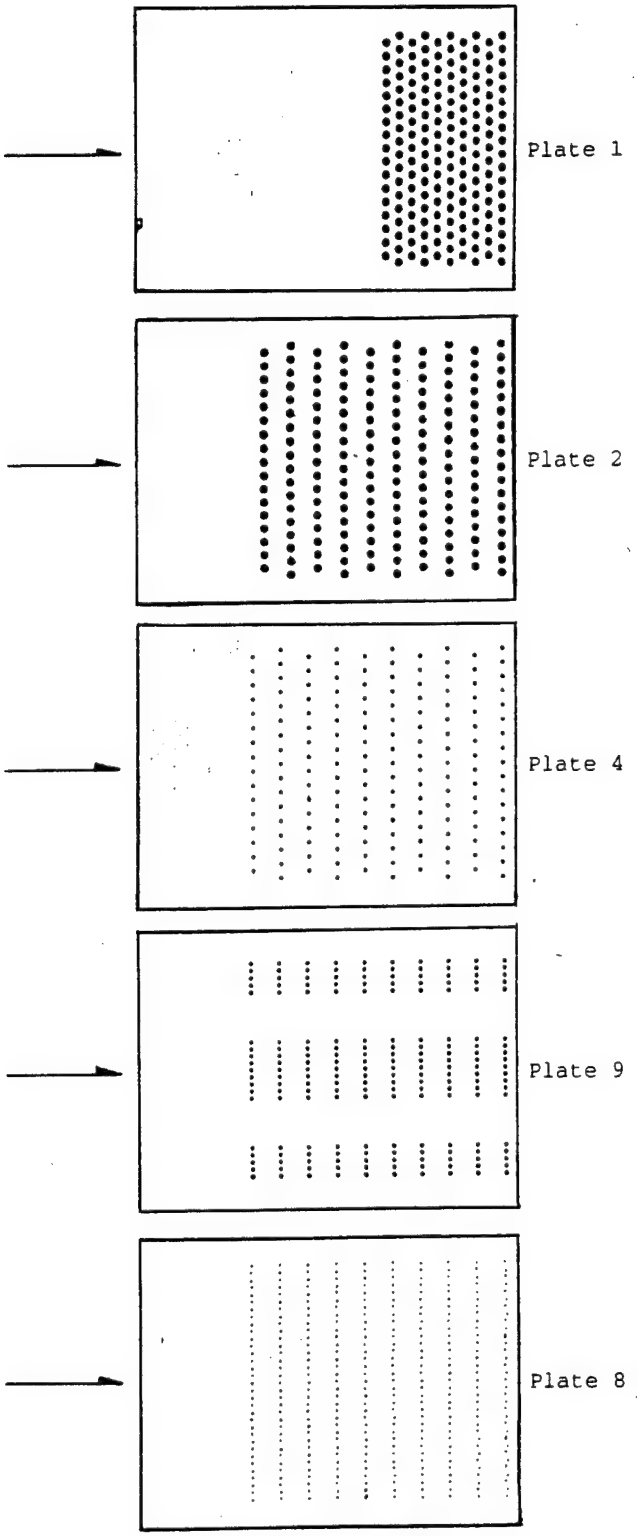

Figure 3. Injection distributions for five selected injection plates.

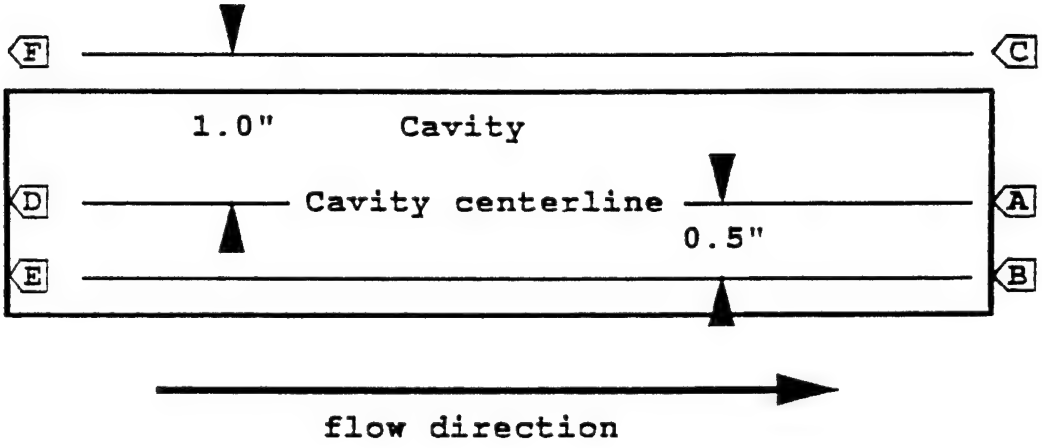

Figure 4. Six stations of the cone probe velocity survey.

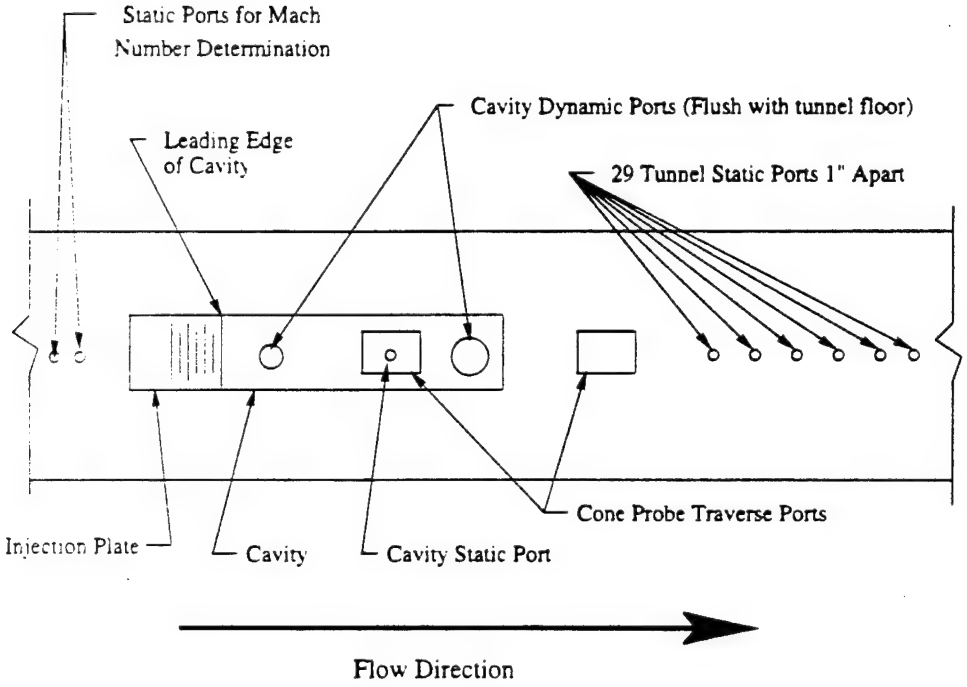

Figure 5. Schematic of the tunnel floor showing the relative placement of the cavity, mass injection, dynamic transducers, cone probe ports, and various other static pressure ports.

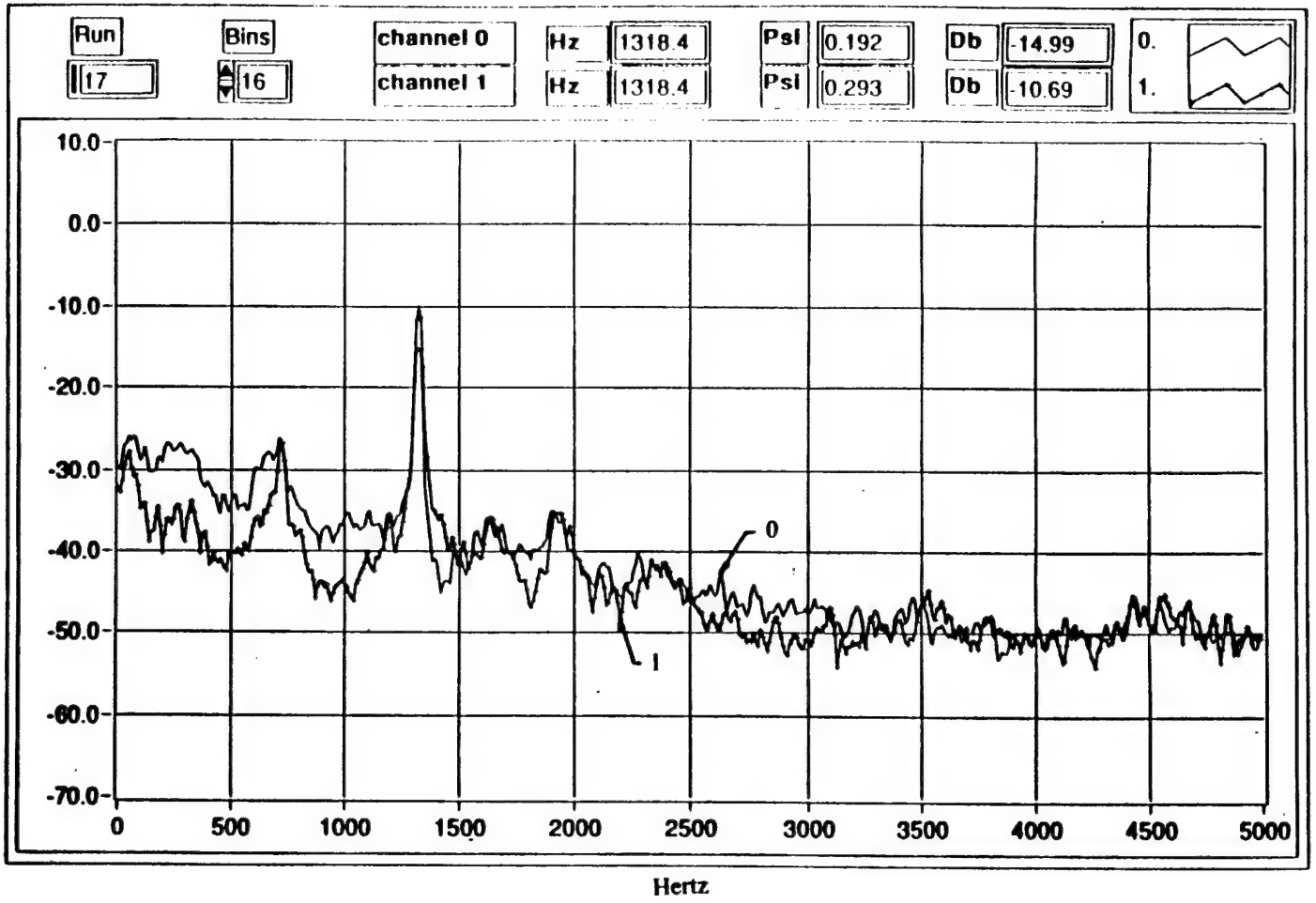

(a) Without mass injection (Baseline)

Figure 6. Spectrum results for Mach 0.5.

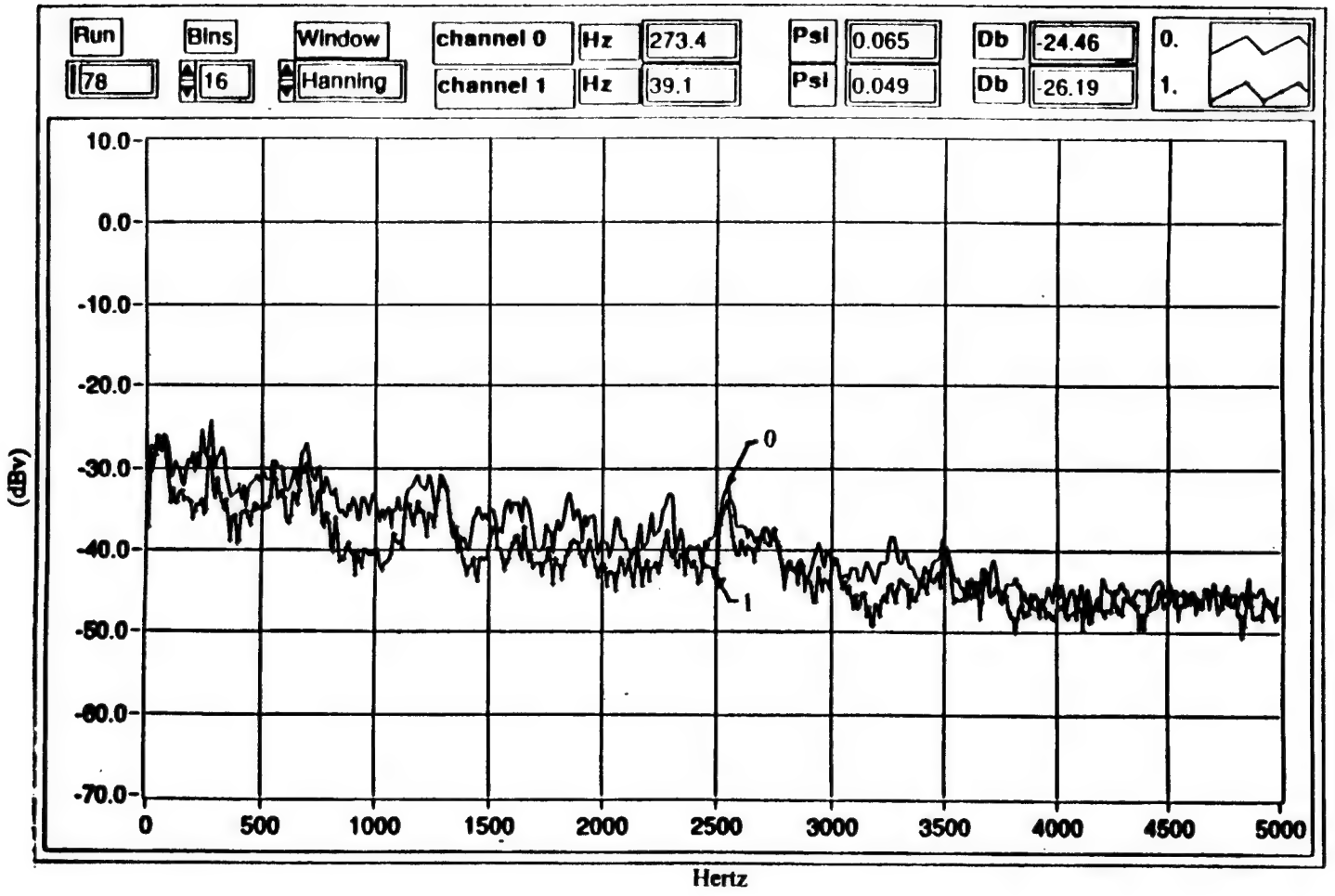

(b) Mach number 0.5 with 0.10 lbm/s mass injection using plate no. 9

Figure 6. (continued)

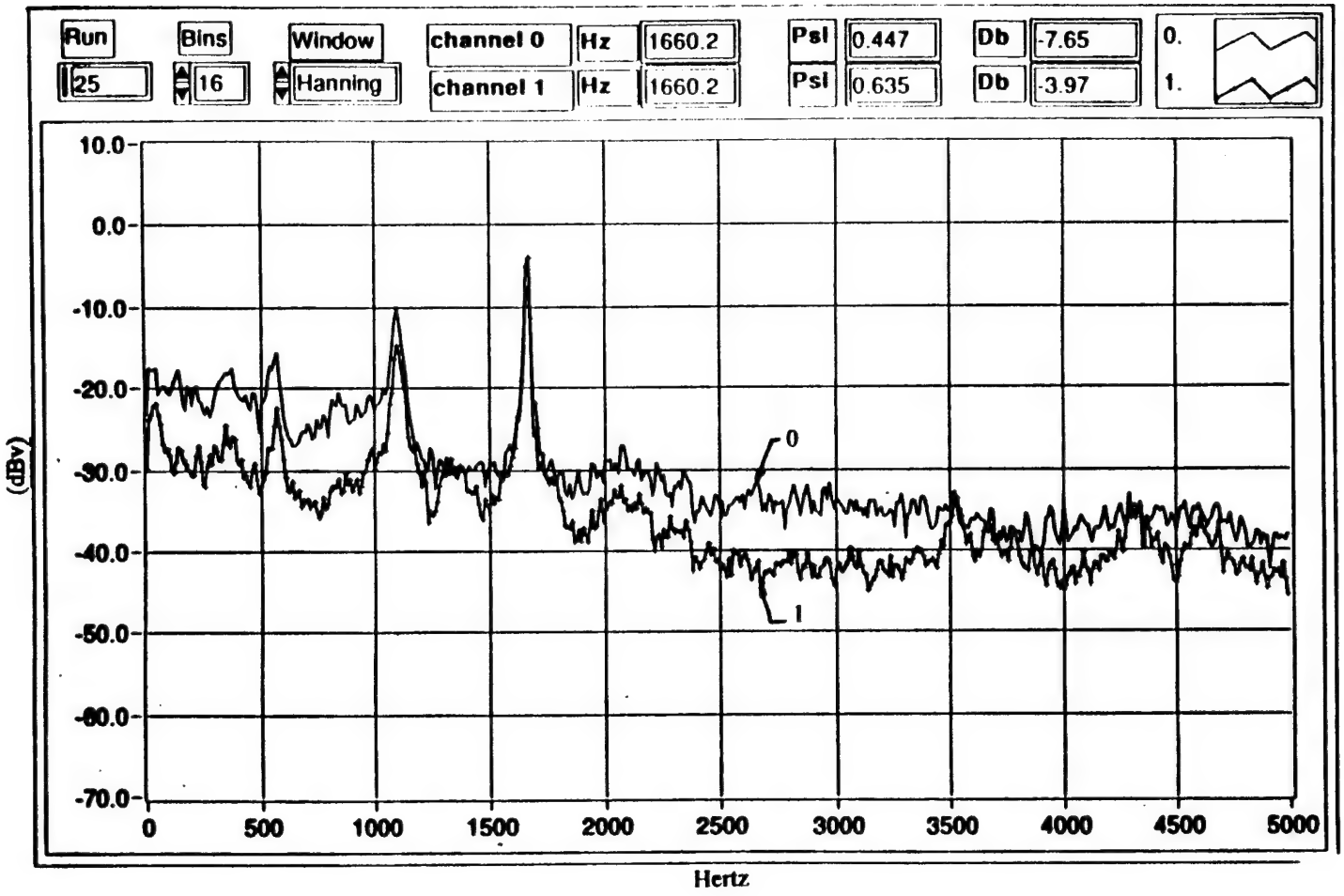

(a) Mach number range between 0.68 and 0.70 with no mass injection (Baseline)

Figure 7. Spectrum results for Mach number 0.7.

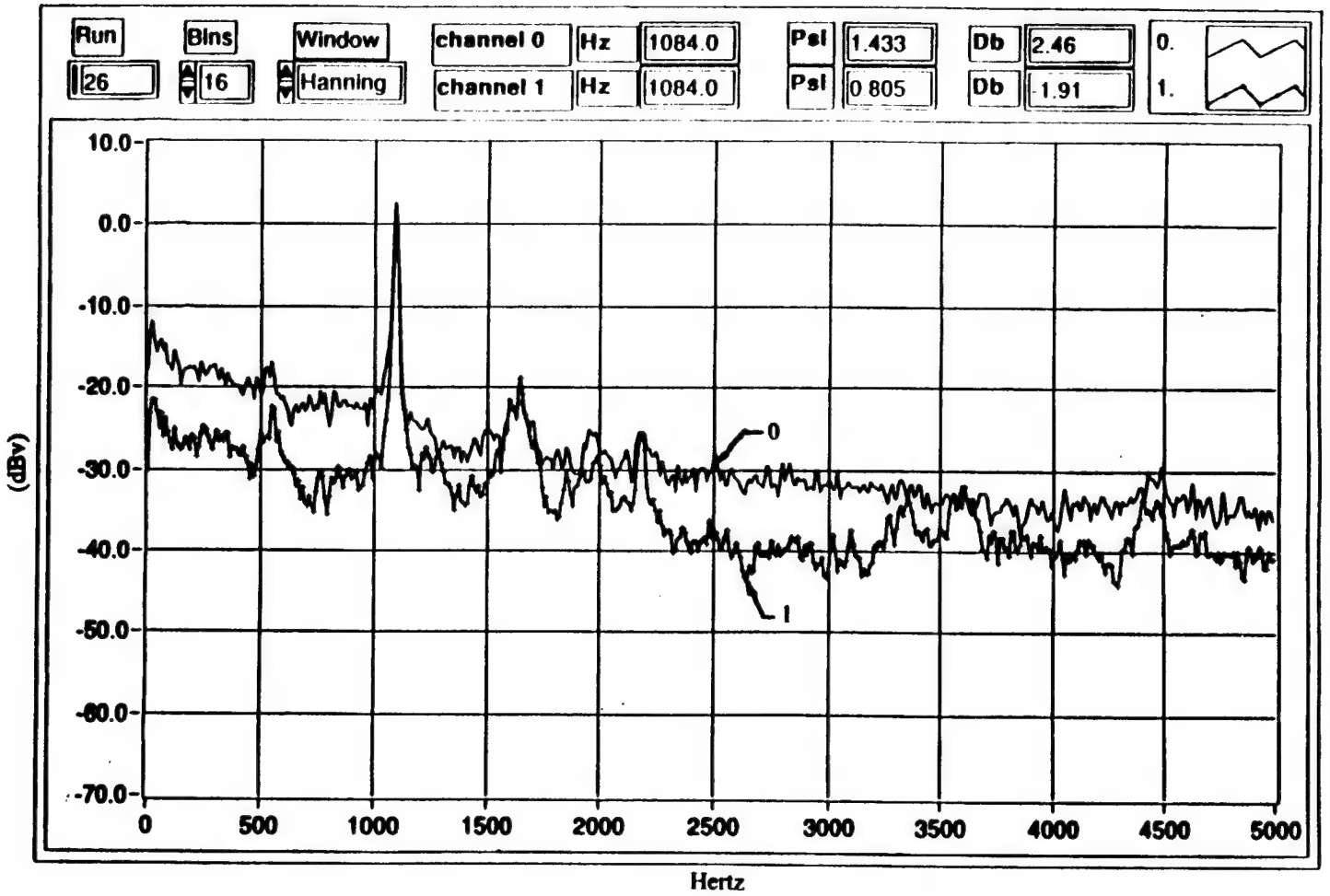

(b) Mach number range between 0.70 and 0.72 with no mass injection (Baseline)

Figure 7. (continued)

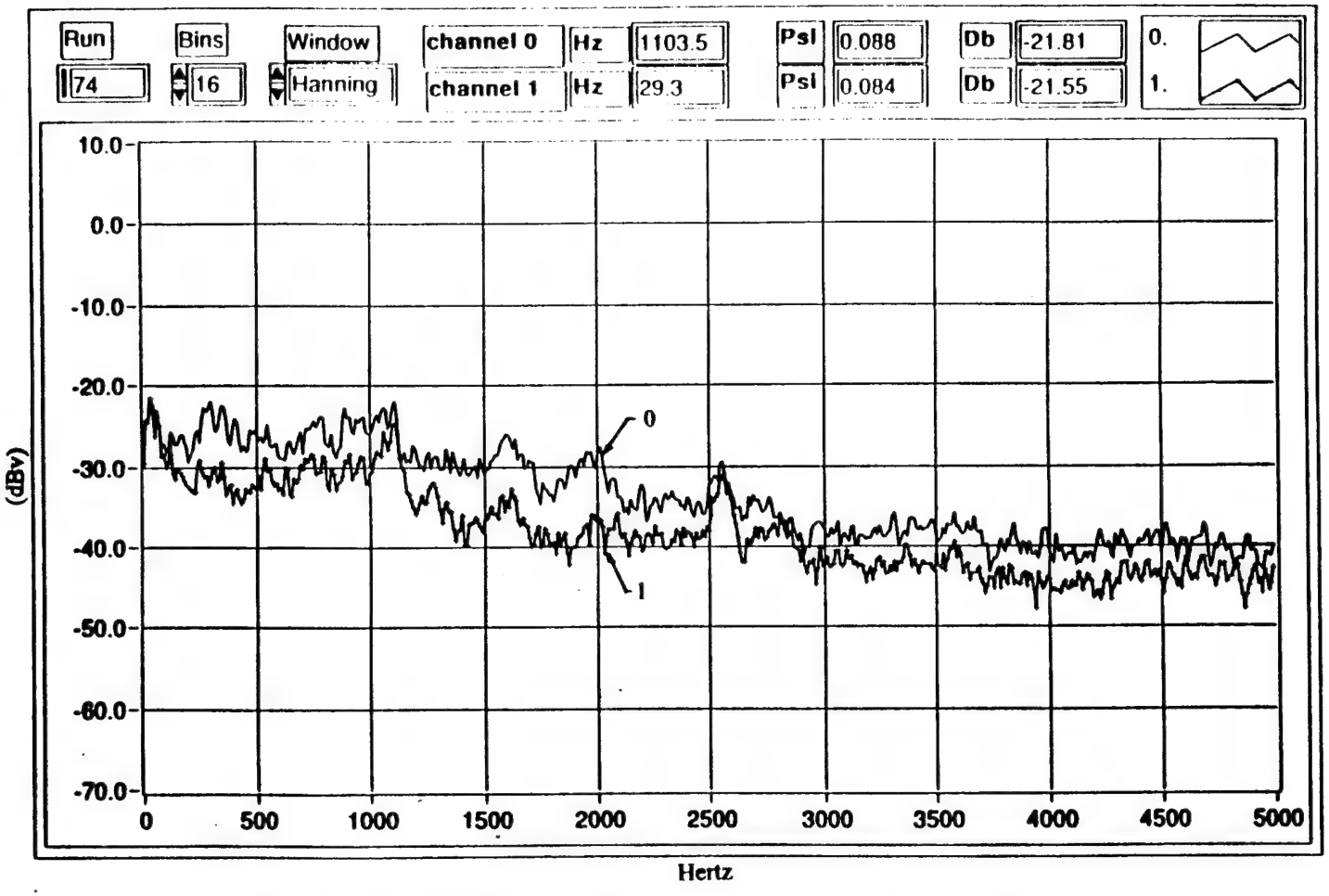

(c) Mach number range between 0.68 and 0.70 with 0.10 lbm/s mass injection using plate 9

Figure 7. (continued)

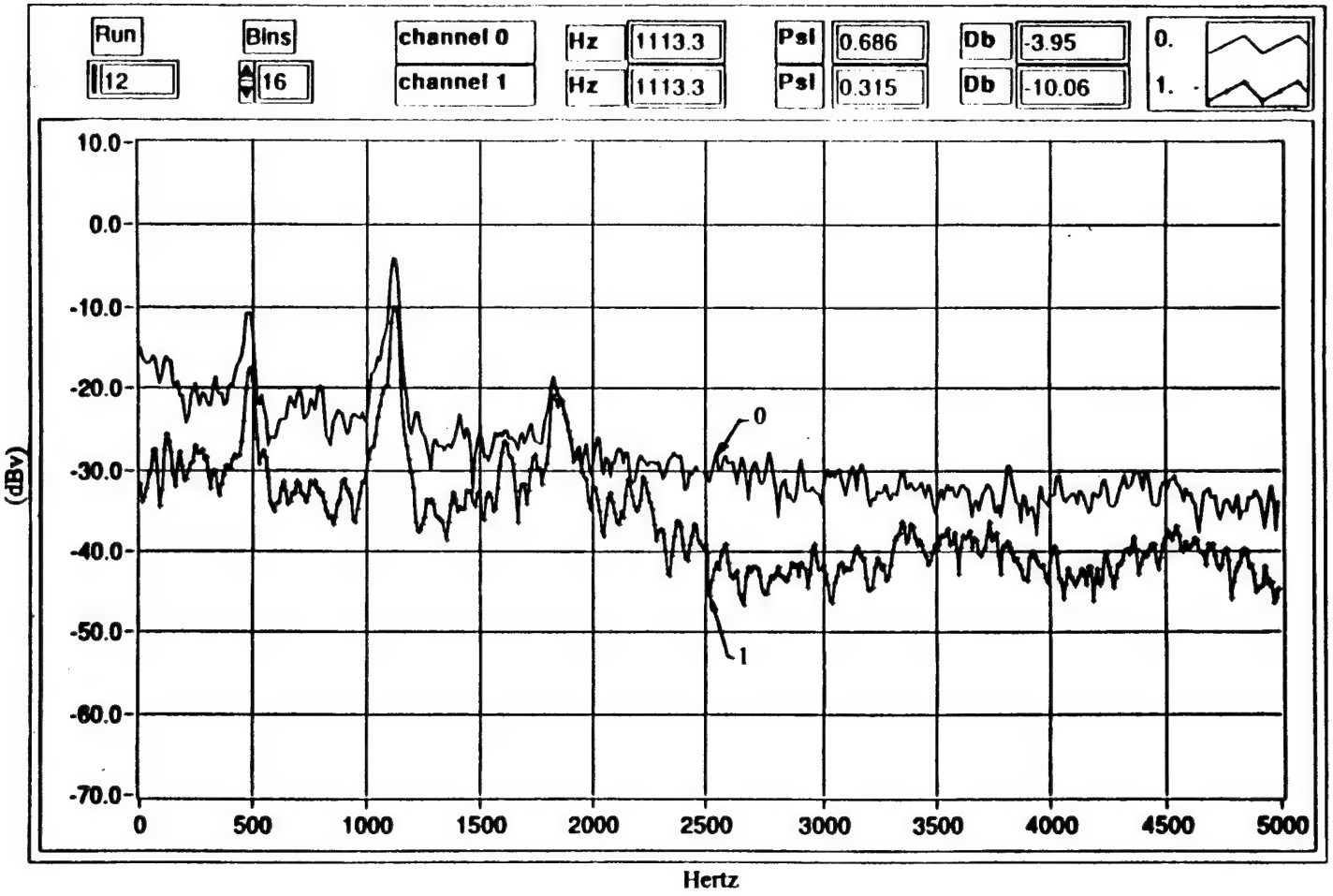

(a) Without mass injection (Baseline)

Figure 8. Spectrum results for Mach number 0.80.

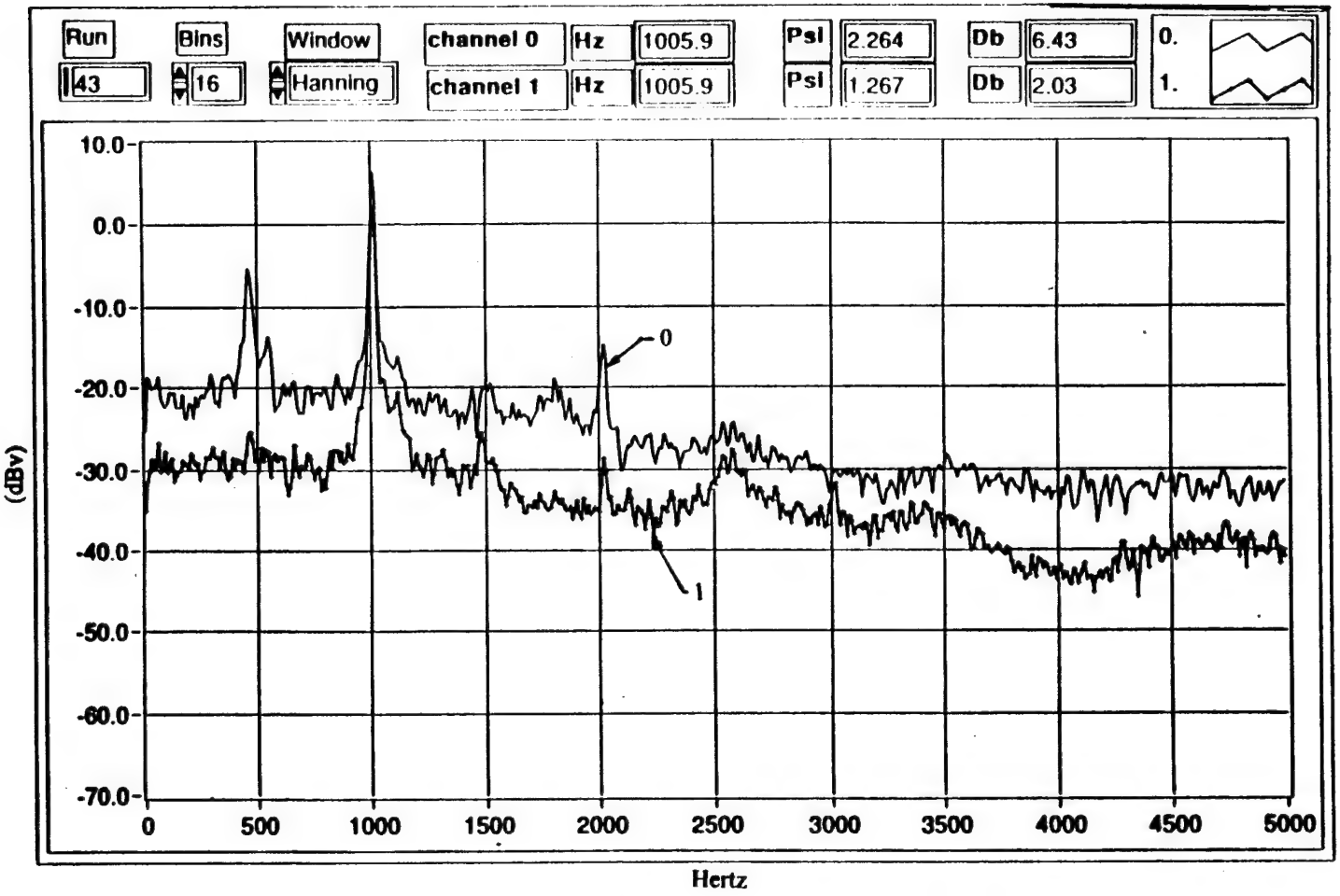

(b) Mach number 0.80 with 0.05 lbm/s mass injection using plate 2

Figure 8. (continued)

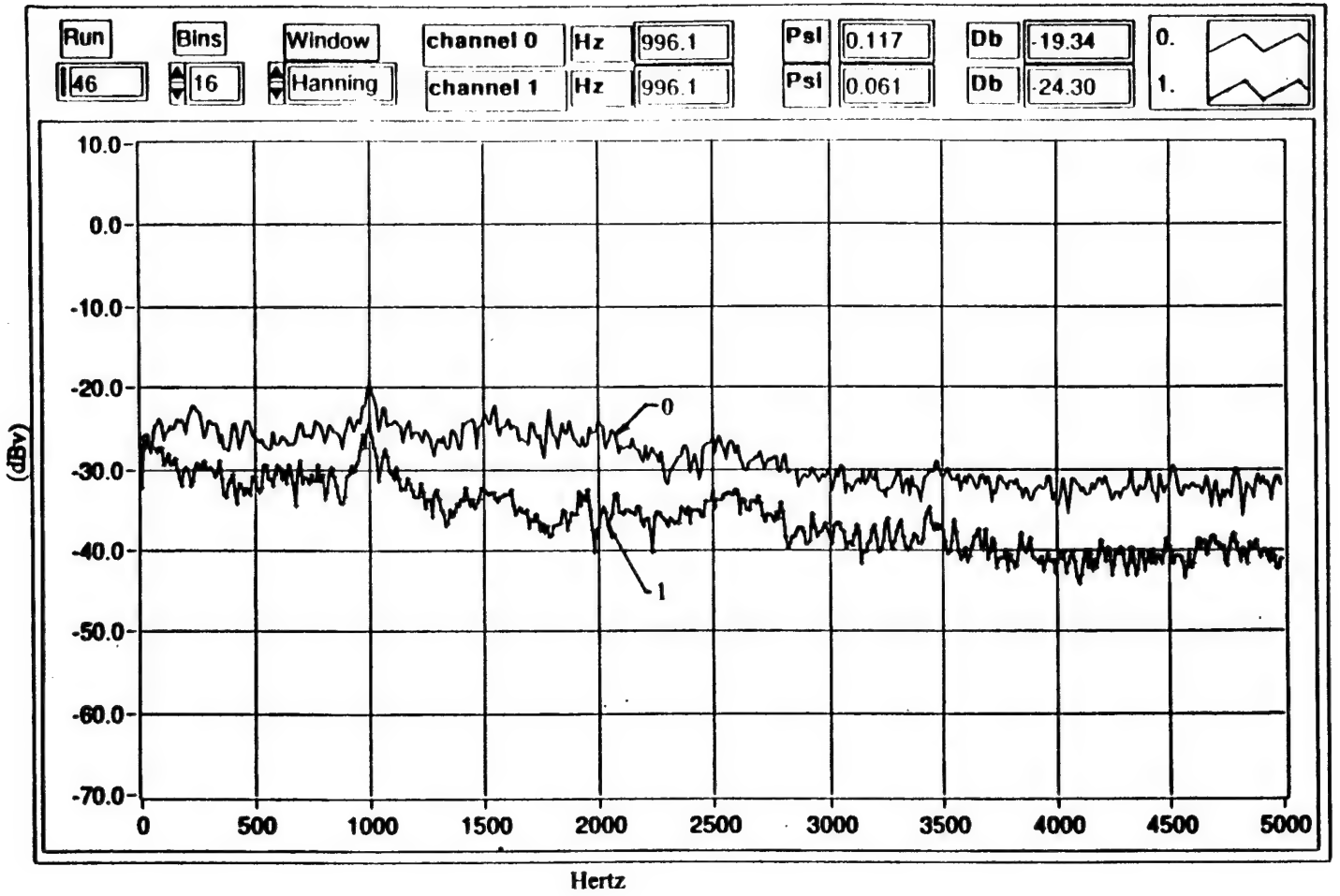

(c) Mach number 0.80 with 0.15 lbm/s mass injection using plate 2

Figure 8. (continued)

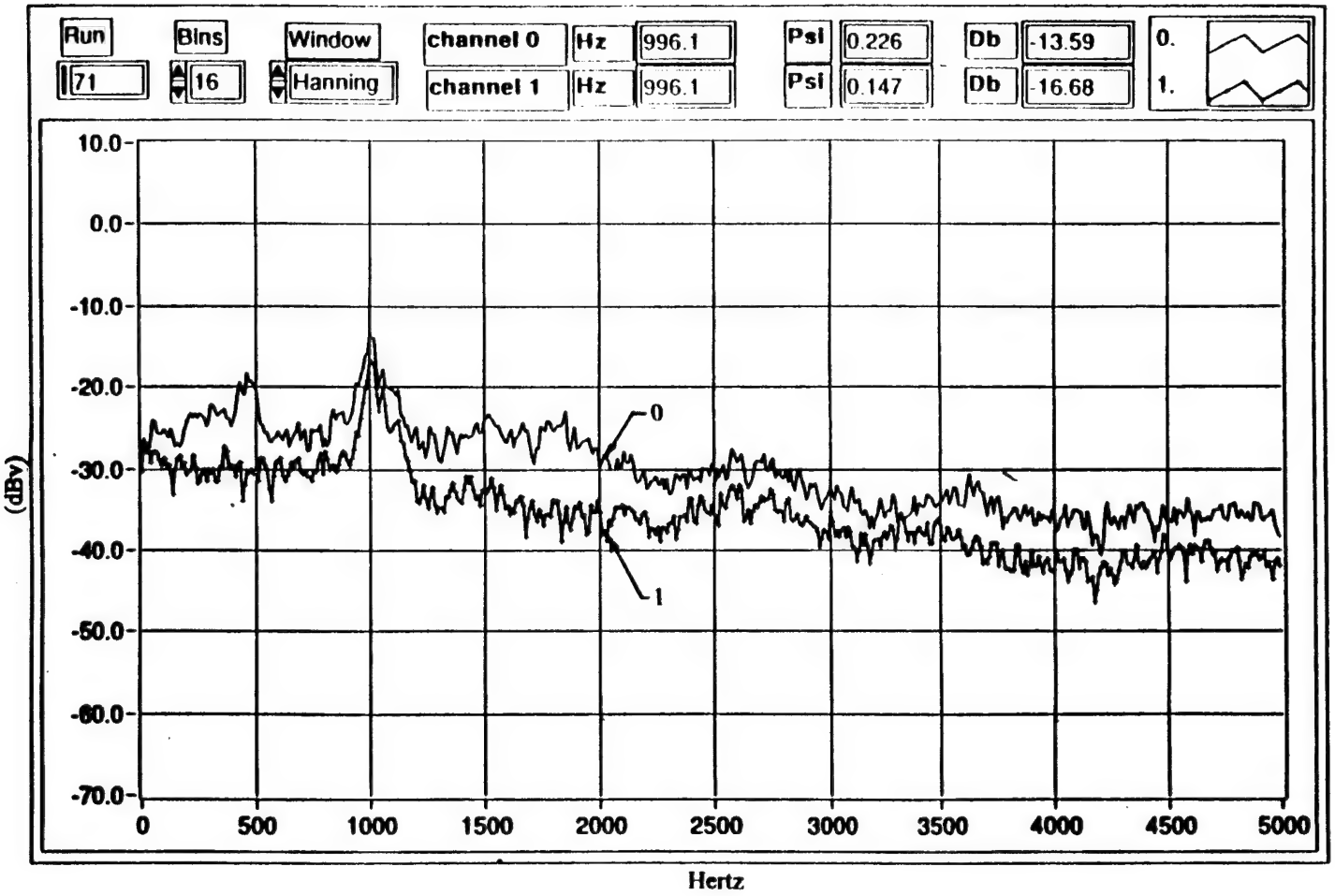

(d) Mach 0.80 with 0.05 lbm/s mass injection using plate 9

Figure 8. (continued)

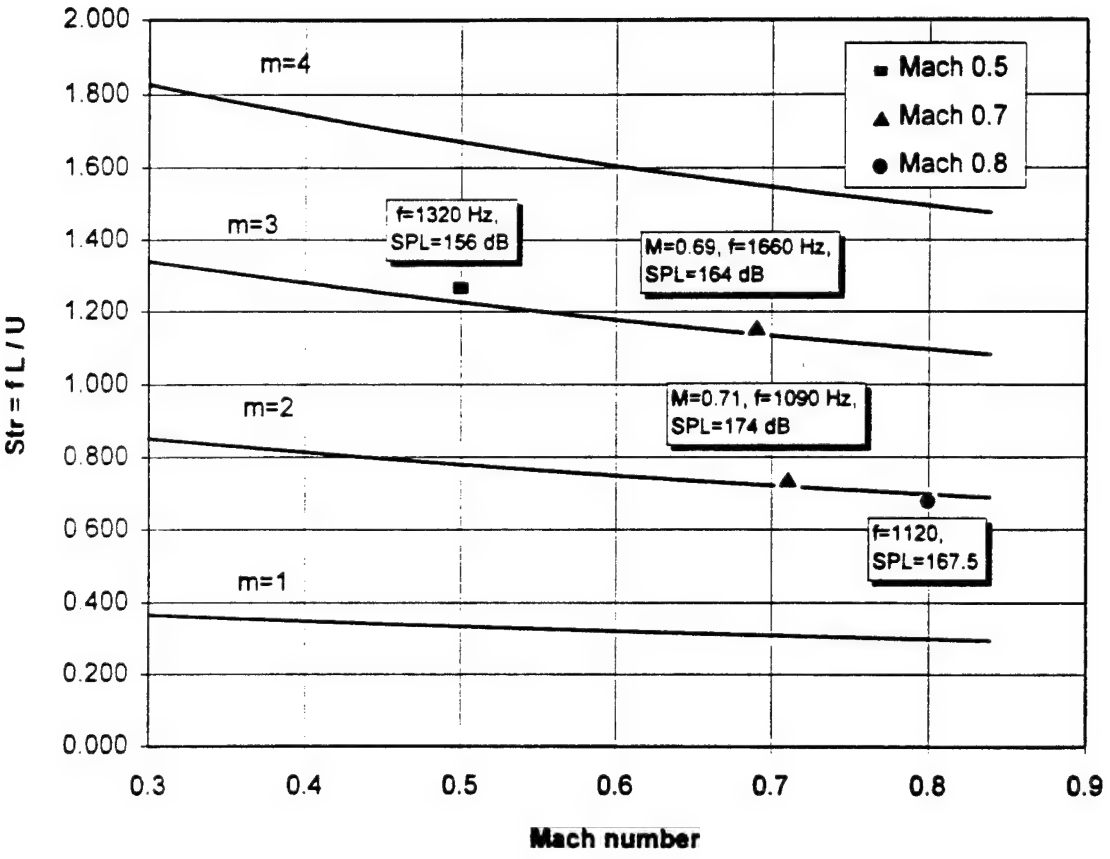

Figure 9. Comparison of experimental baseline peak amplitude frequencies to peak amplitude frequencies predicted by the modified Rossiter's equation.

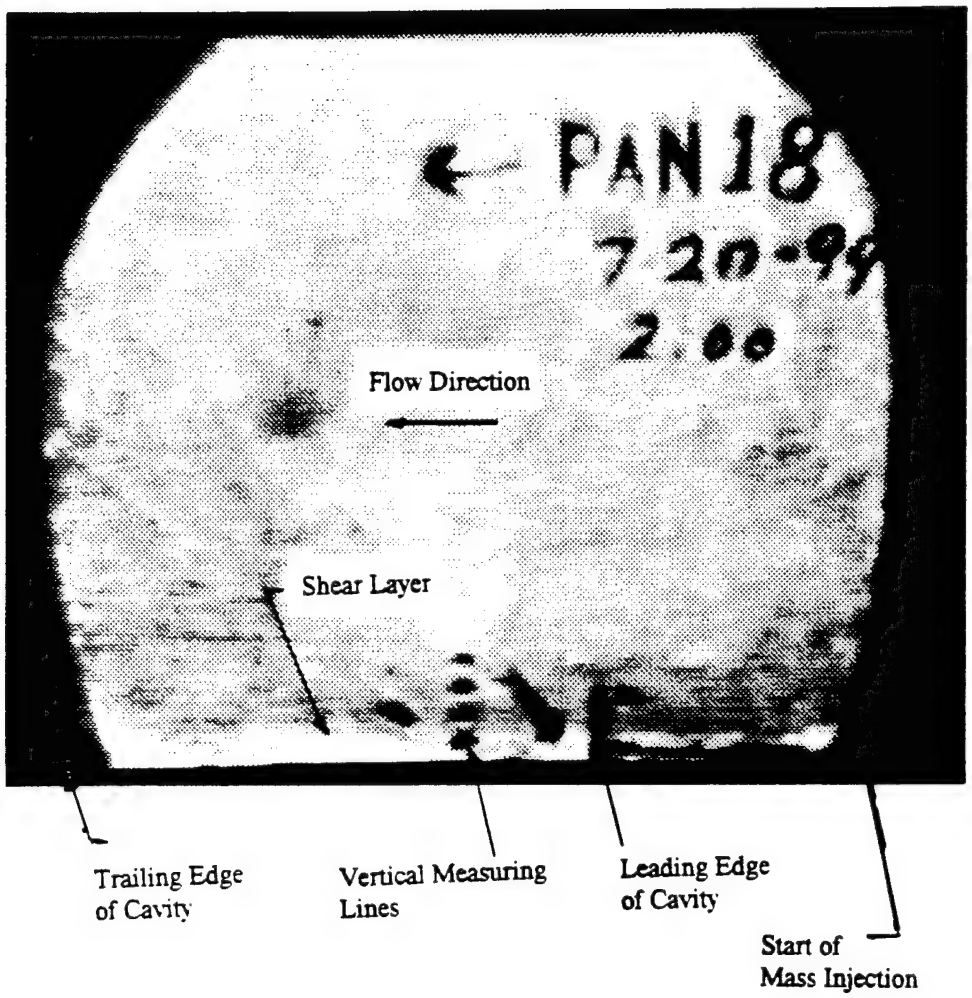

Figure 10. Schlieren photograph of the boundary and shear layers over the cavity at Mach 0.7 and no mass injection.

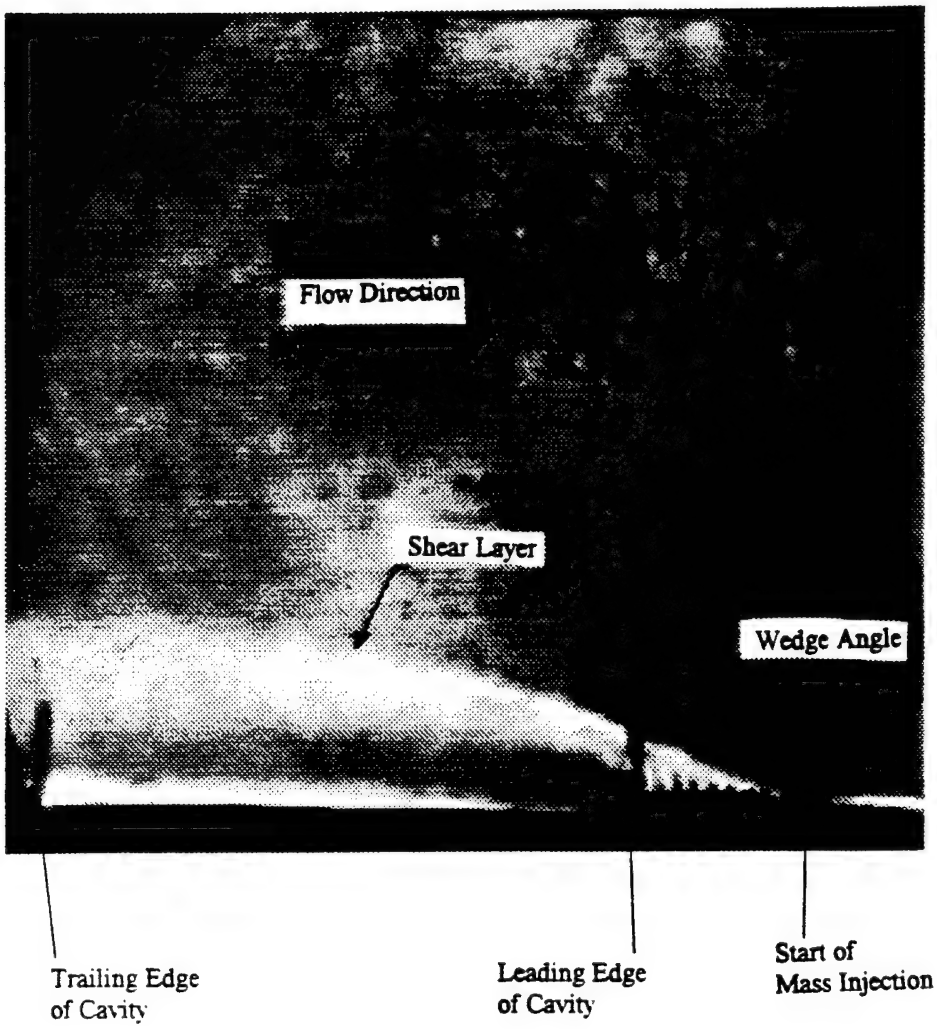

Figure 11. Schlieren photograph of boundary and shear layers over a cavity at Mach 0.7 and 0.10 lbm/s mass injection using plate 4.

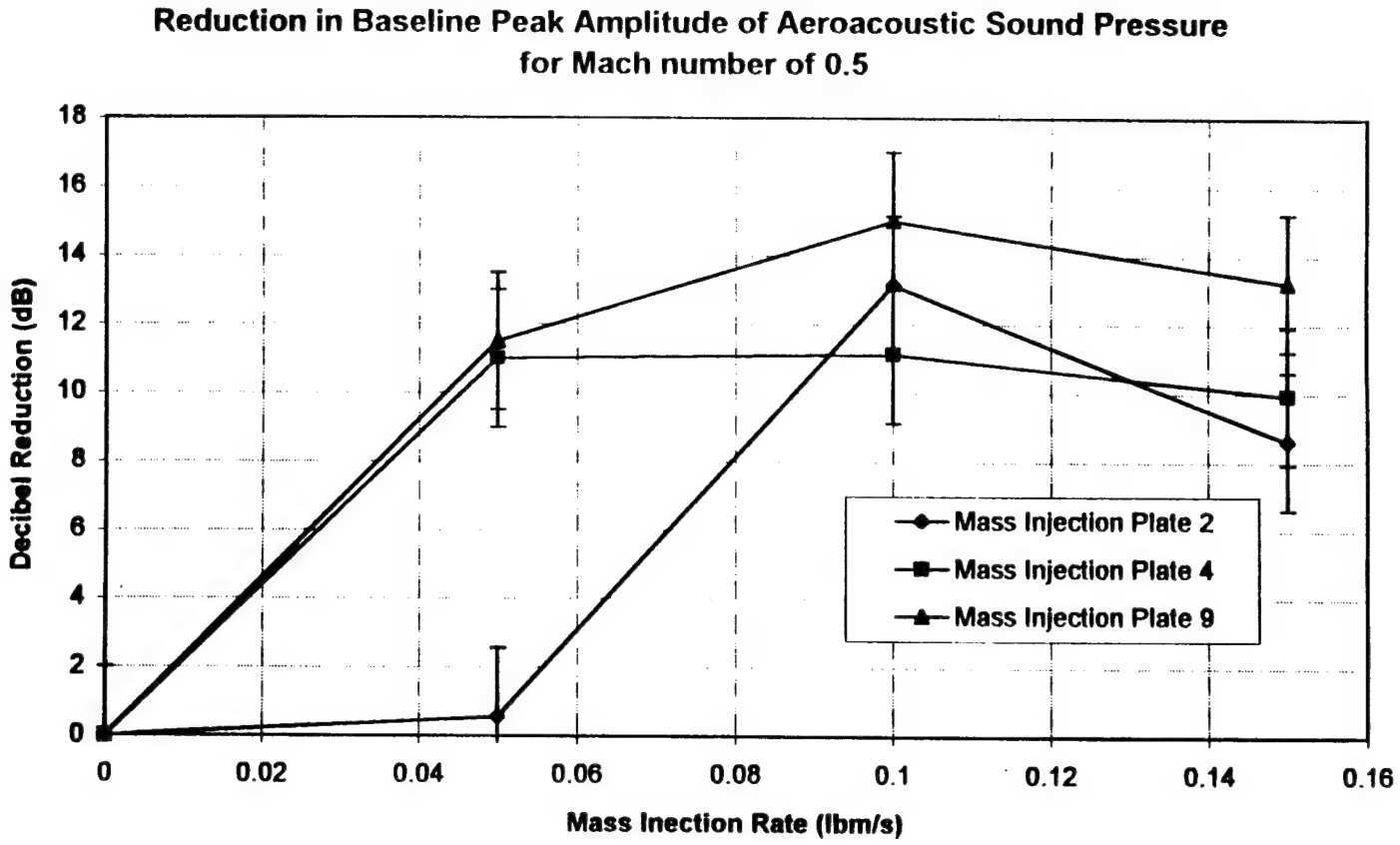

Figure 12. Plot of sound pressure level reduction for Mach number 0.5 versus mass injection rate for plates 2, 4, and 9.

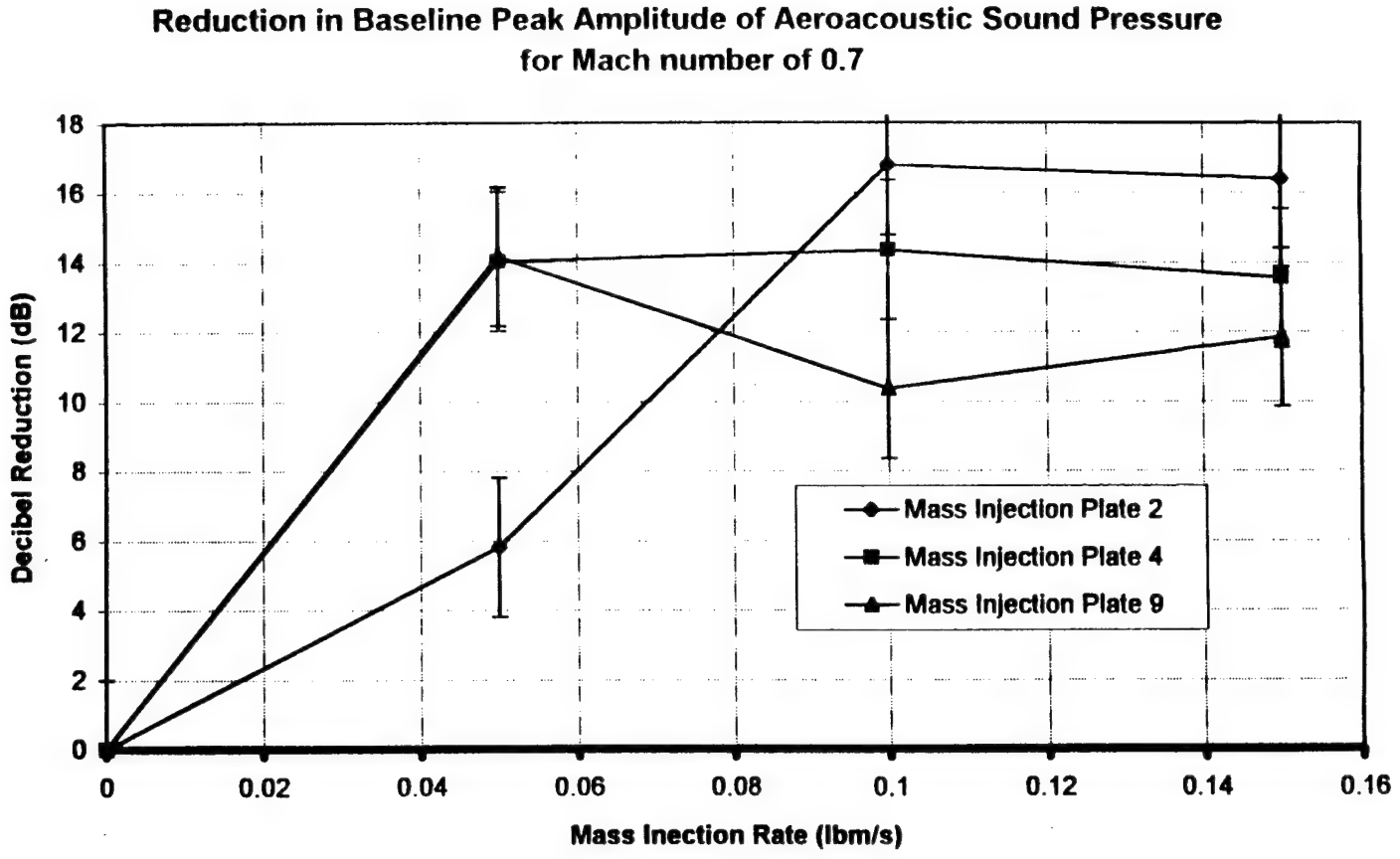

Figure 13. Plot of sound pressure level reduction for Mach number 0.7 versus mass injection rate for plates 2, 4, and 9.

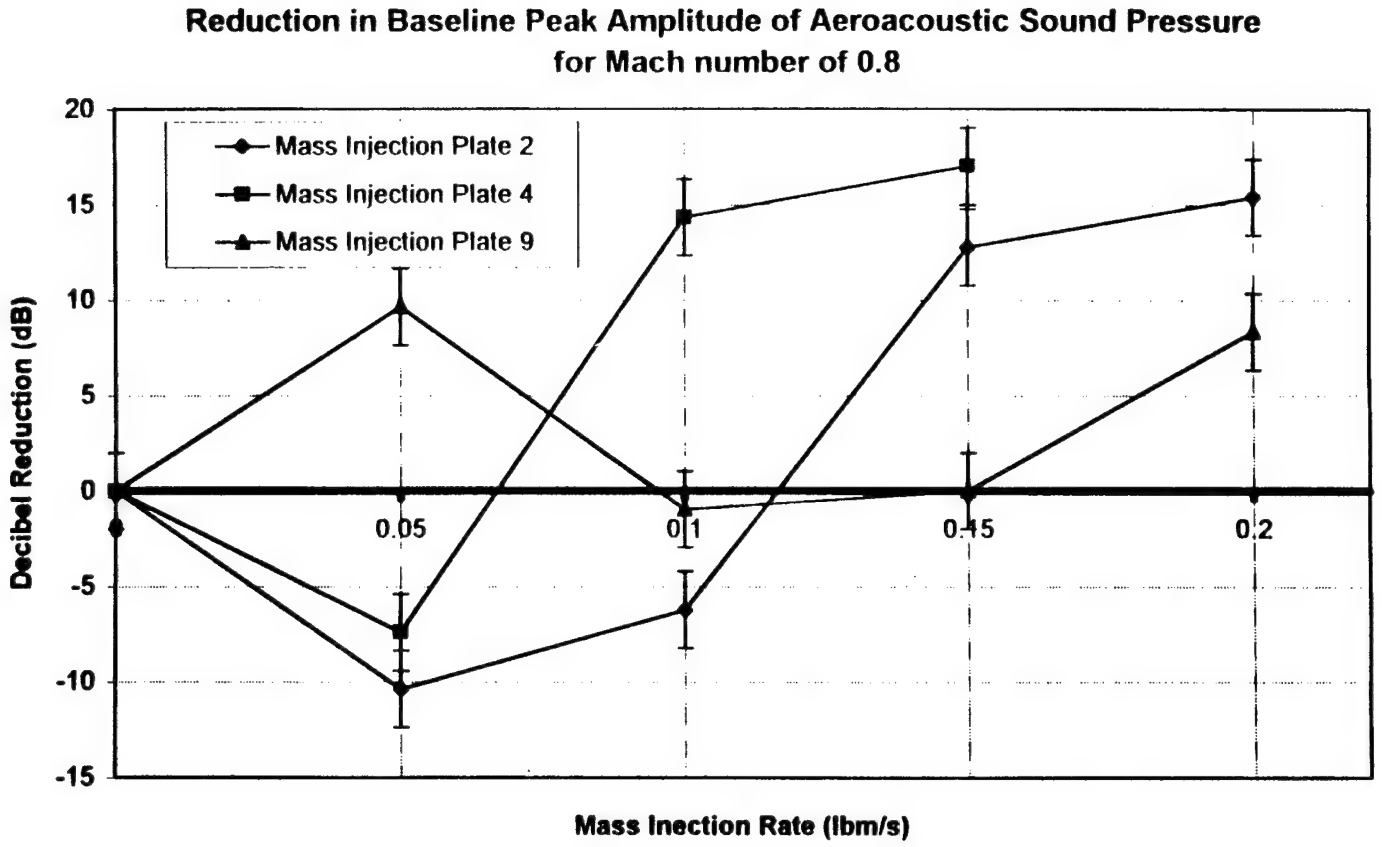

Figure 14. Plot of sound pressure level reduction for Mach number 0.8 versus mass injection rate for plates 2, 4, and 9.

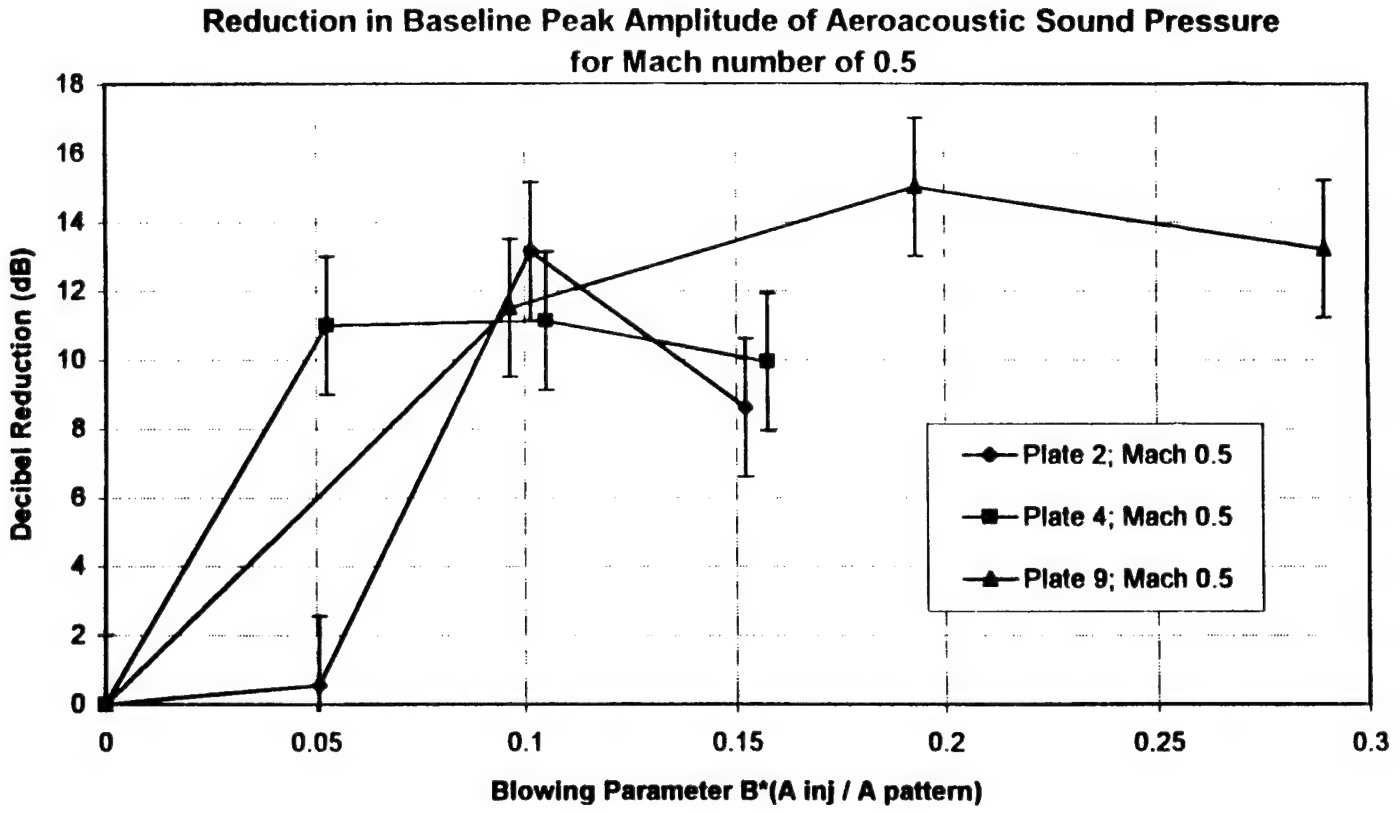

Figure 15. Plot of sound pressure level reduction for Mach number 0.5 versus blowing parameter $B^*(A_{inj}/A_{pattern})$ for plates 2, 4, and 9.

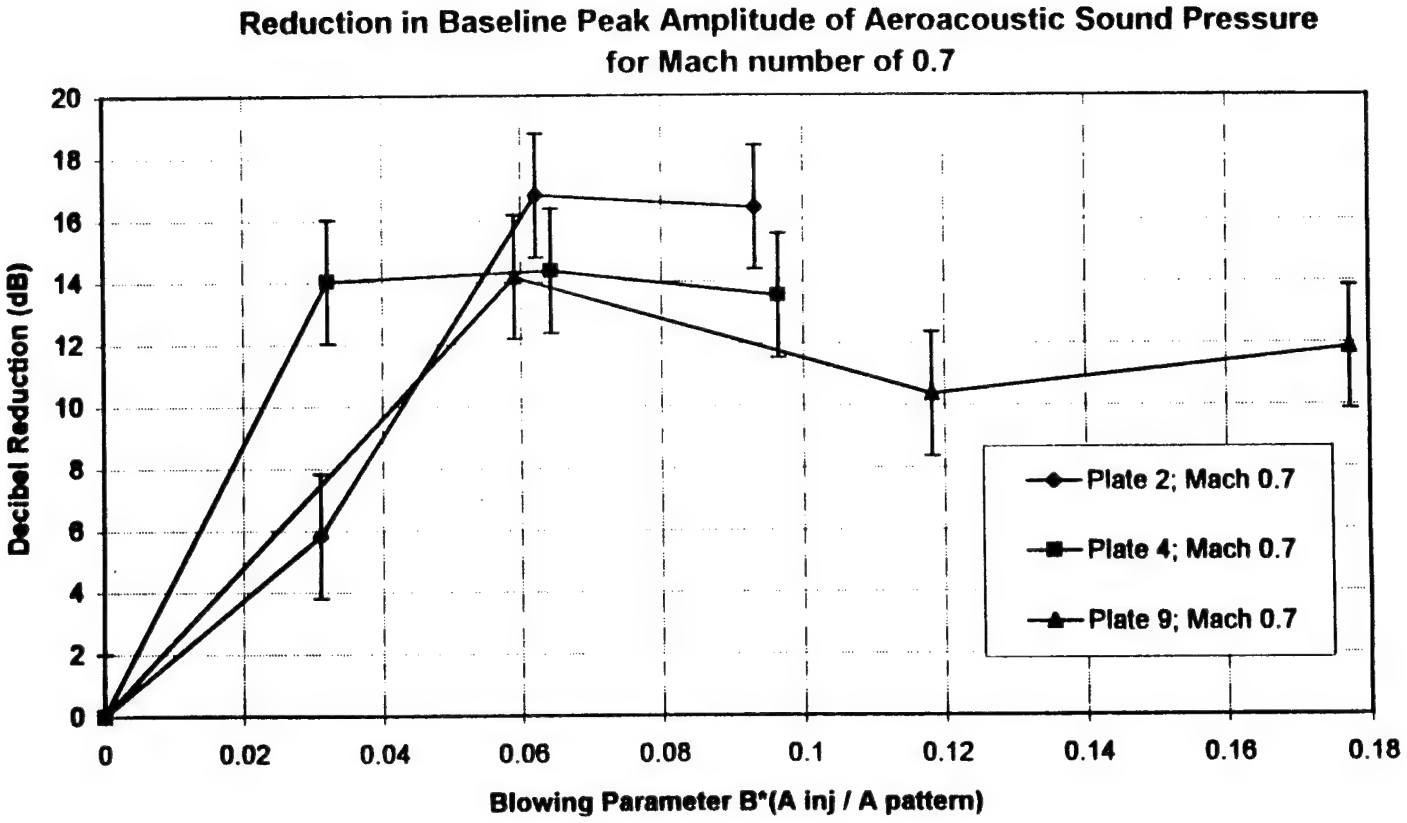

Figure 16. Plot of sound pressure level reduction for Mach number 0.7 versus blowing parameter $B^*(A_{inj}/A_{pattern})$ for plates 2, 4, and 9.

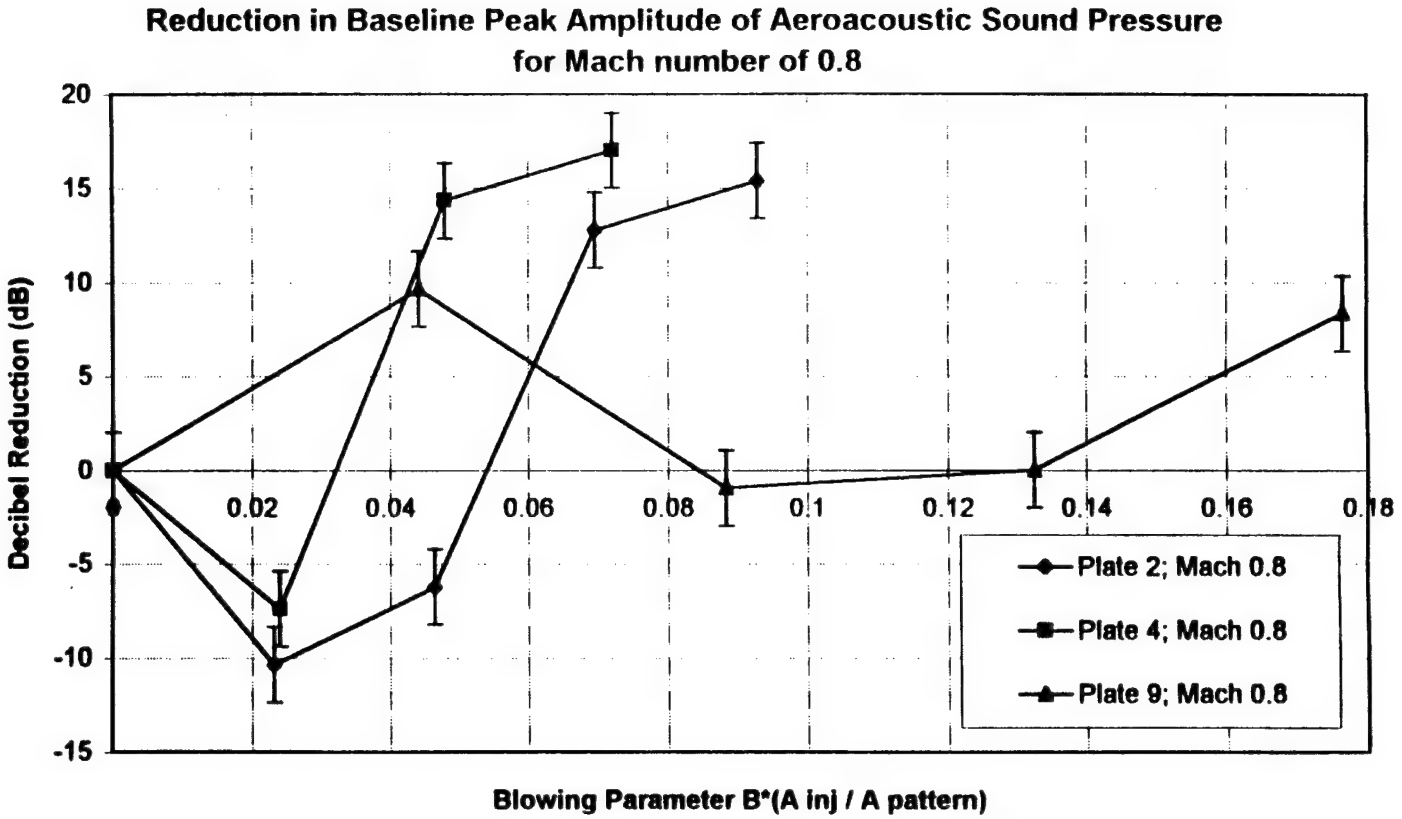

Figure 17. Plot of sound pressure level reduction for Mach number 0.8 versus blowing parameter $B^*(A_{inj}/A_{pattern})$ for plates 2, 4, and 9.

Table I. Summary of maximum amplitude reduction of Aeroacoustic Sound Pressure Level for plates 2, 4, and 9 at Mach numbers of 0.5, 0.7, and 0.8.

Mach 0.5	Plate #	Mass Injection Rate	Blowing Parameter B*(Area inj / Area Cavity)	Amplitude Reduction (dB)
	2	0.1	0.1015	13.15
	4	0.1	0.1050	11.12
	9	0.1	0.1931	15
Mach 0.7	**Plate #**	**Mass Injection Rate**	**Blowing Parameter B*(Area inj / Area Cavity)**	**Amplitude Reduction (dB)**
	2	0.1	0.0622	16.78
	4	0.1	0.0643	14.35
	9	0.05	0.0591	14.16
Mach 0.8	**Plate #**	**Mass Injection Rate**	**Blowing Parameter B*(Area inj / Area Cavity)**	**Amplitude Reduction (dB)**
	2	0.2	0.0929	15.39
	4	0.15	0.0721	17
	9	0.05	0.0441	9.64

Table II. Typical supersonic data.

Plate	mass flow (lbm/s)	Peak Amplitudes (Psi)	(dB)	B	B_c ($X10^3$)	B_d ($X10^3$)
2	0.00	1.64	175	0.00	0.00	0.00
2	0.03	0.80	169	0.18	5.09	16.3
2	0.05	0.37	162	0.30	8.49	27.2
2	0.10	0.06	146	0.62	17.5	56.0
9	0.00	1.93	176	0.00	0.00	0.00
9	0.05	0.13	153	0.48	7.18	22.9
9	0.10	0.10	151	0.95	14.2	45.4
9	0.15	0.12	152	1.41	21.1	67.5
8	0.00	1.46	174	0.00	0.00	0.00
8	0.03	0.23	158	0.78	5.37	17.2
8	0.05	0.08	149	1.29	8.87	28.4
8	0.10	0.07	148	2.69	18.5	59.2

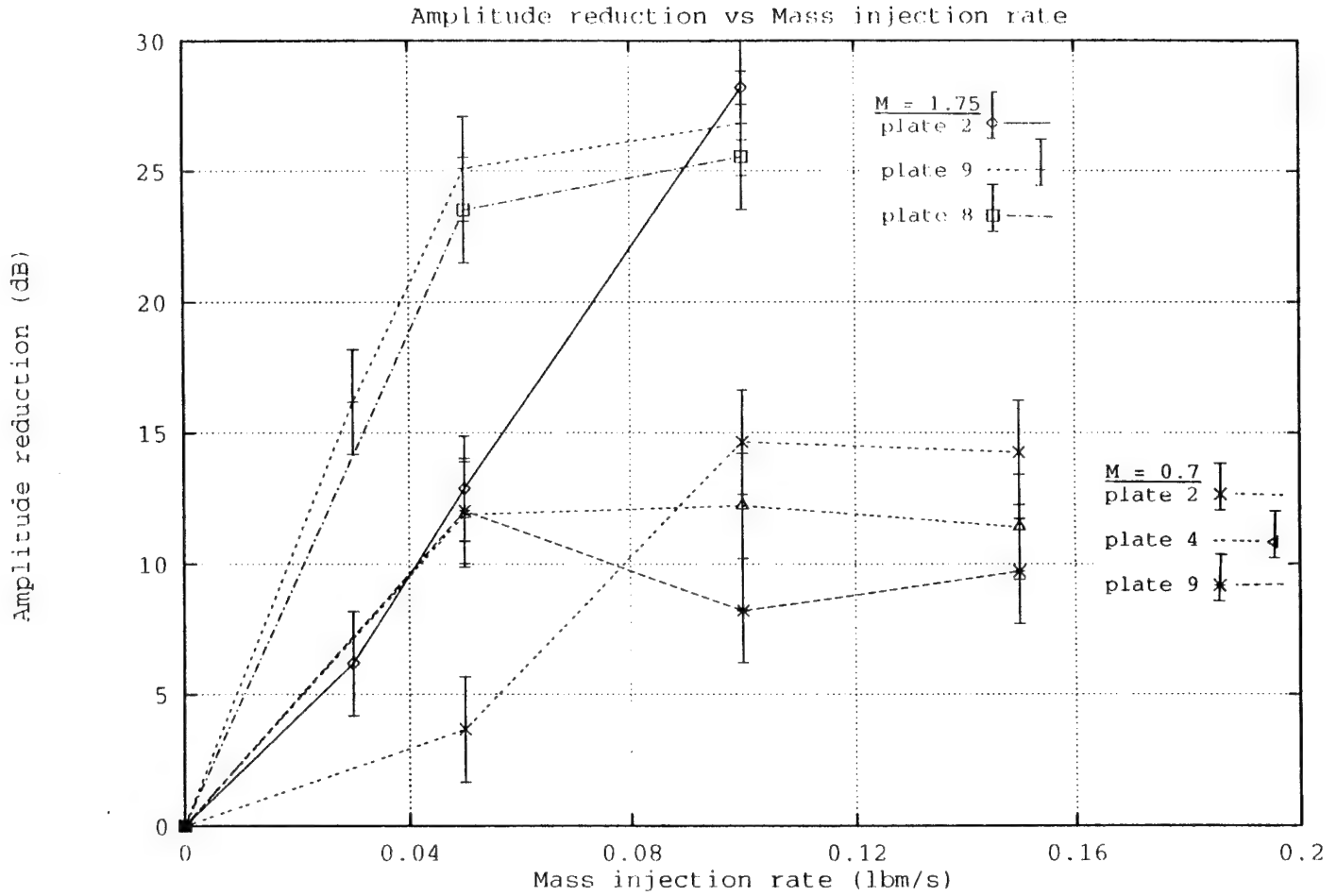

Figure 18. Peak amplitude reduction versus mass injection.

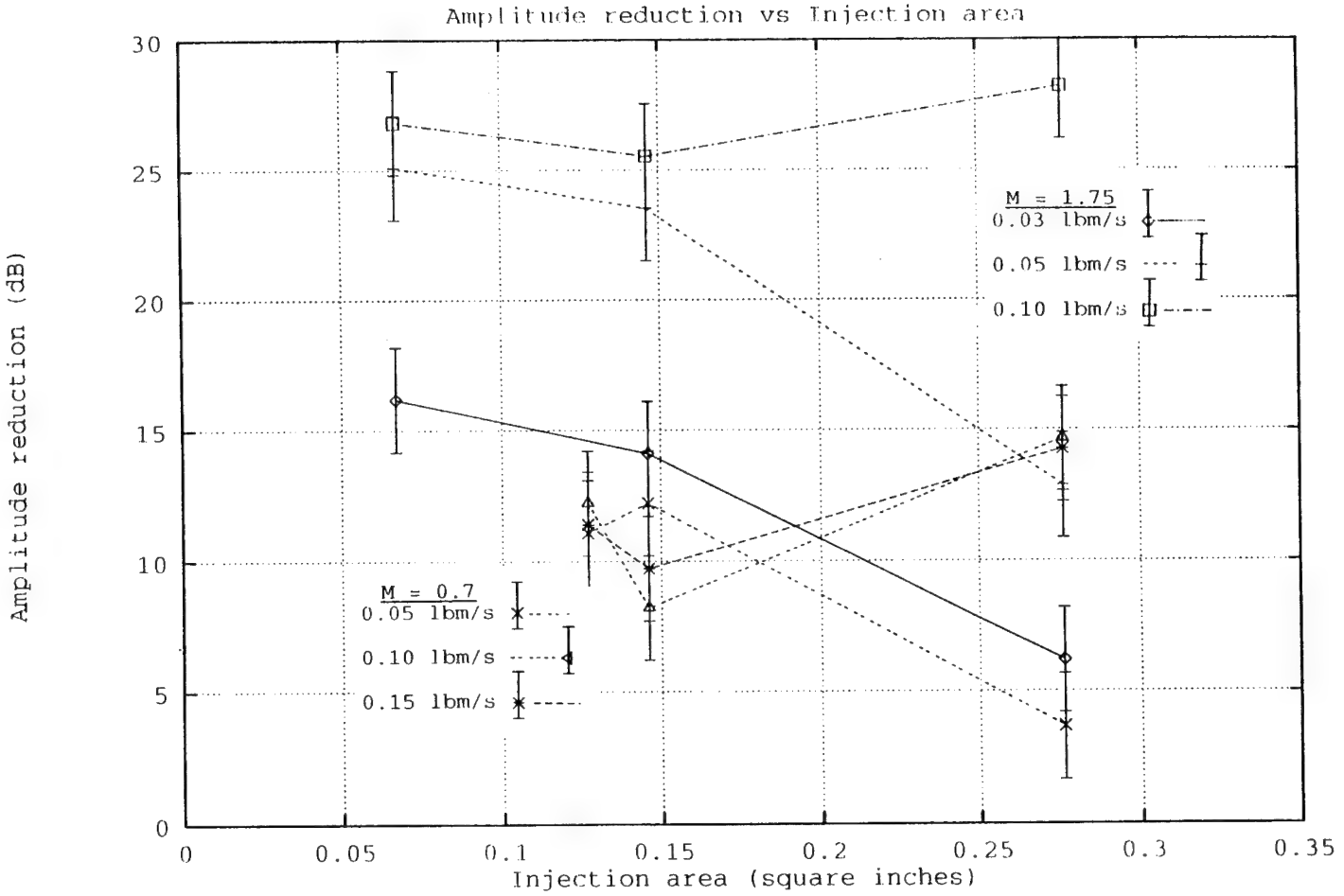

Figure 19. Peak amplitude reduction versus injection area.

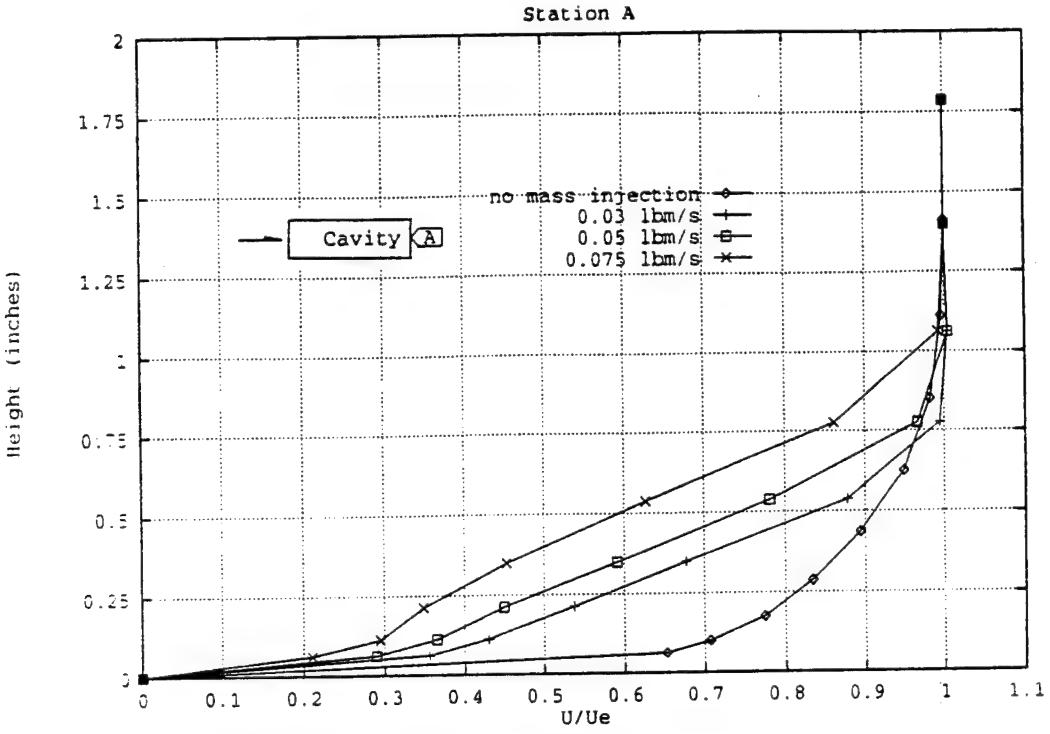

Figure 20. Velocity profiles at station A.

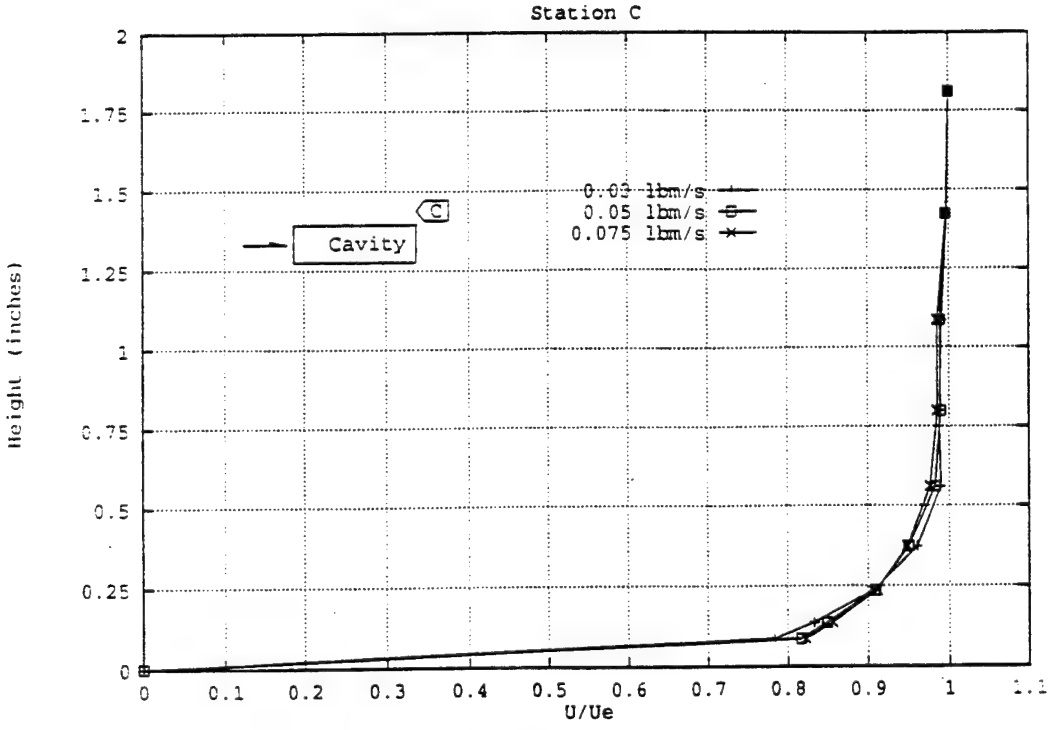

Figure 21. Velocity profiles at station C.

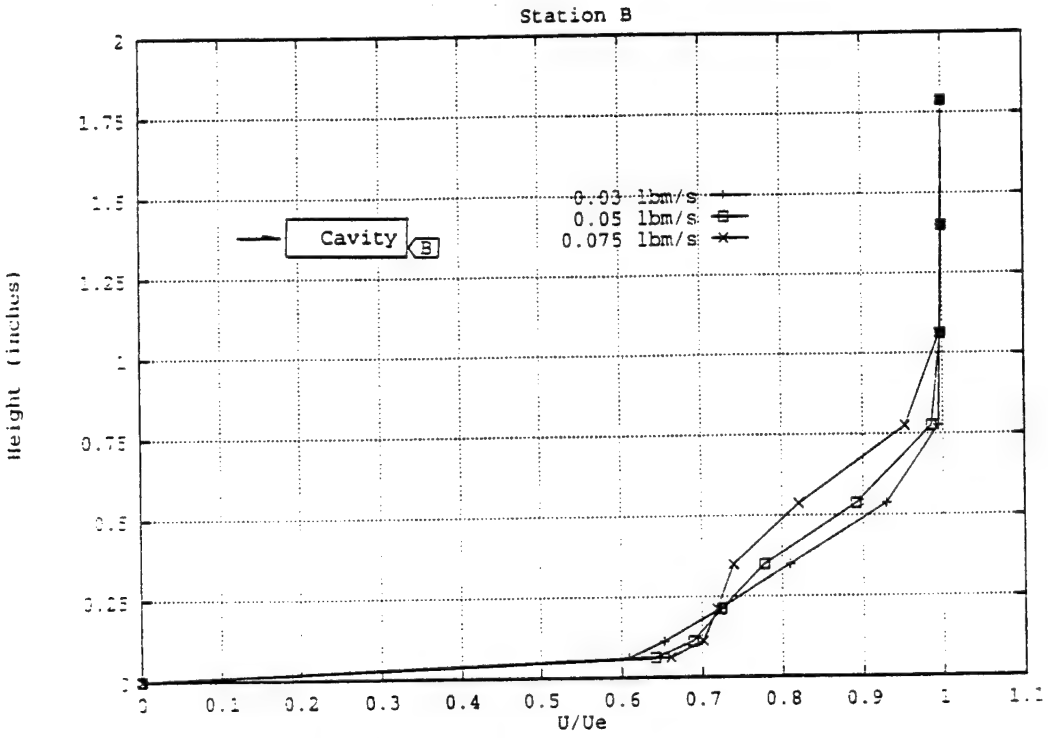

Figure 22. Velocity profiles at station B.

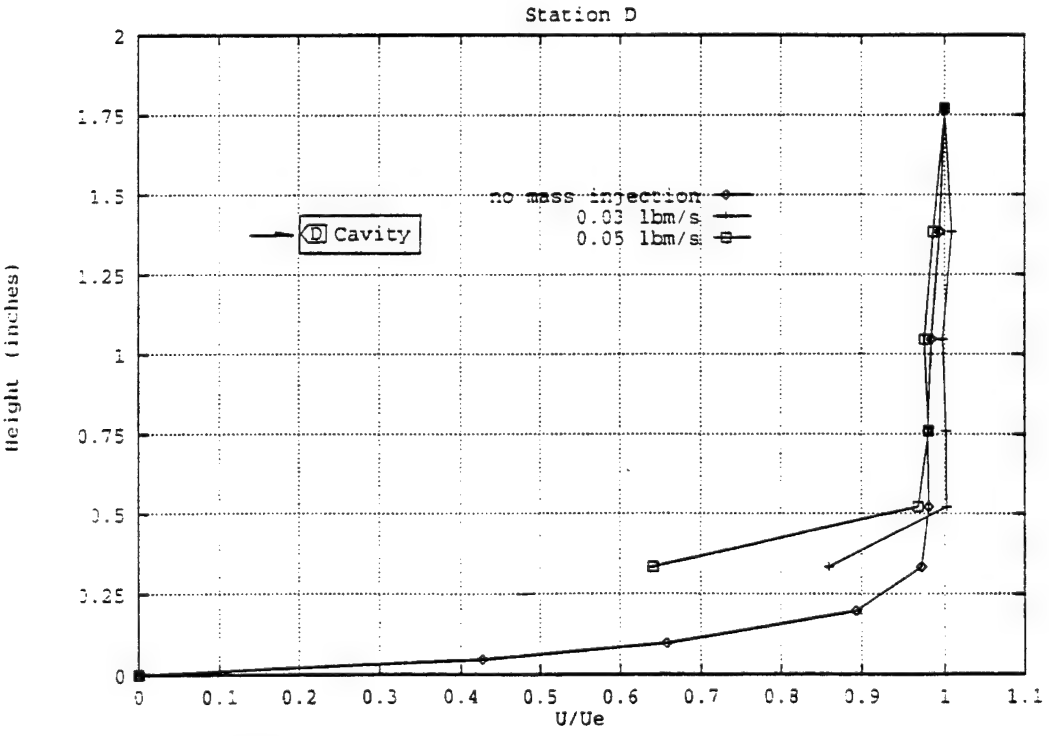

Figure 23. Velocity profiles at station D.

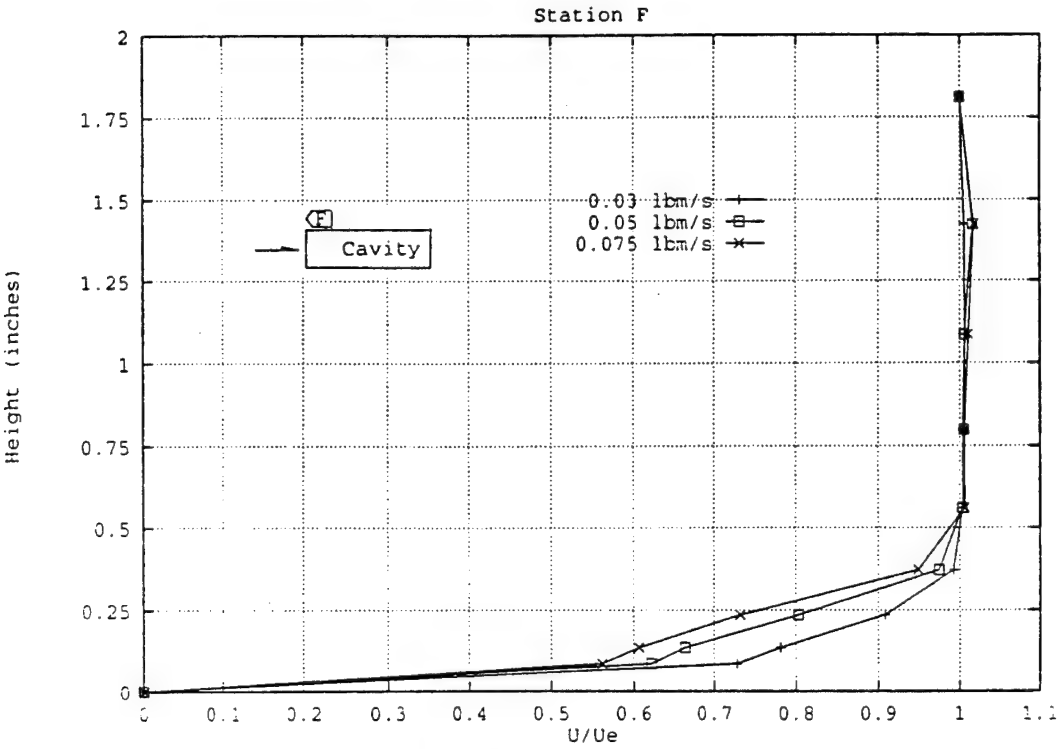

Figure 24. Velocity profiles at station F.

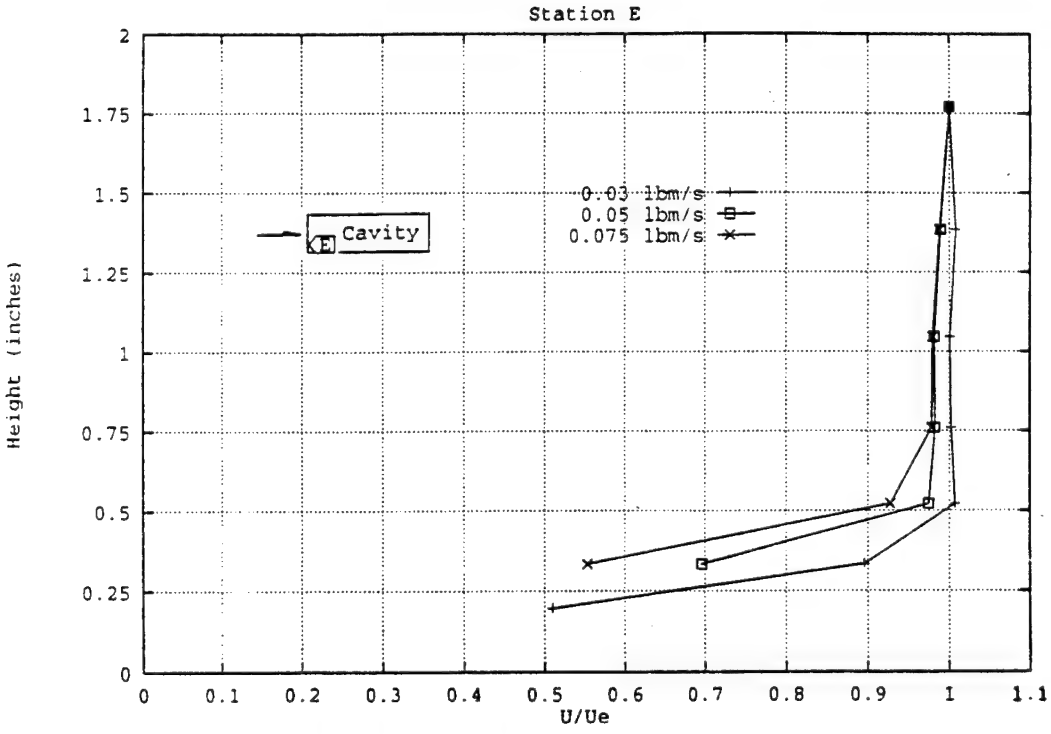

Figure 25. Velocity profiles at station E.

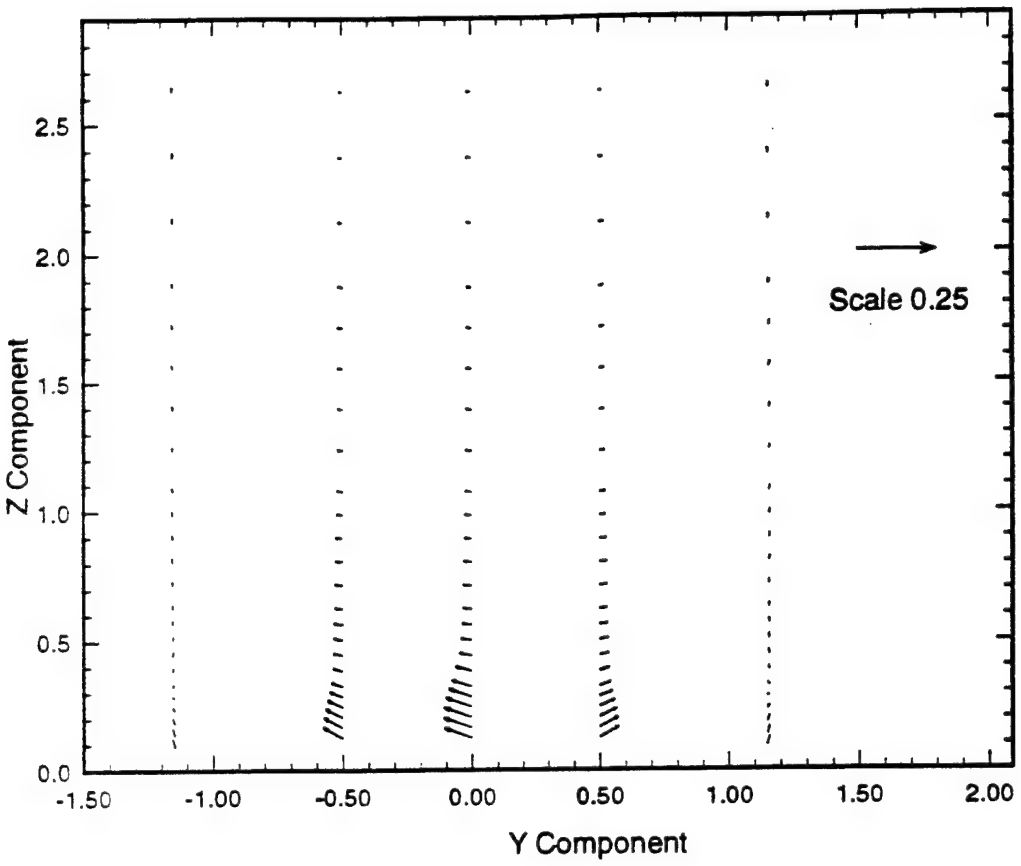

Figure 26. Cone Probe velocity vector plots at the cavity's leading edge for Mach number of 0.7 and no mass injection.

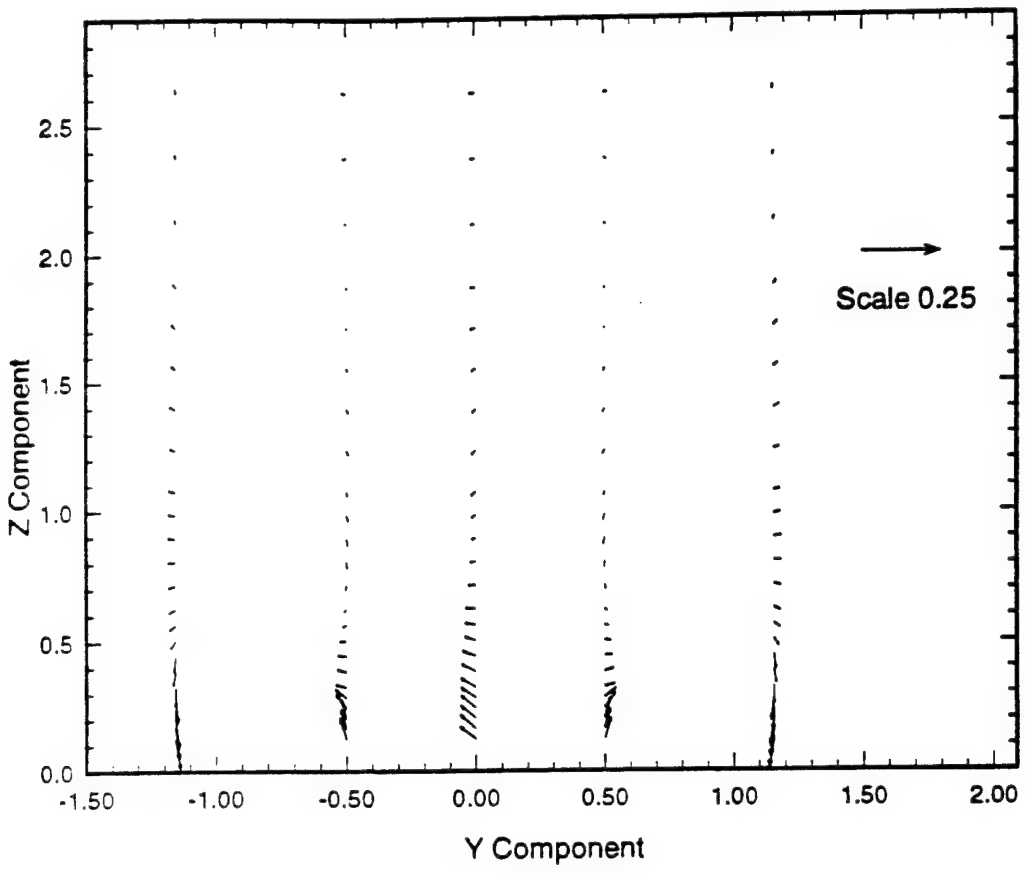

Figure 27. Cone Probe velocity vector plots at the cavity's trailing edge for Mach number of 0.7 and no mass injection.

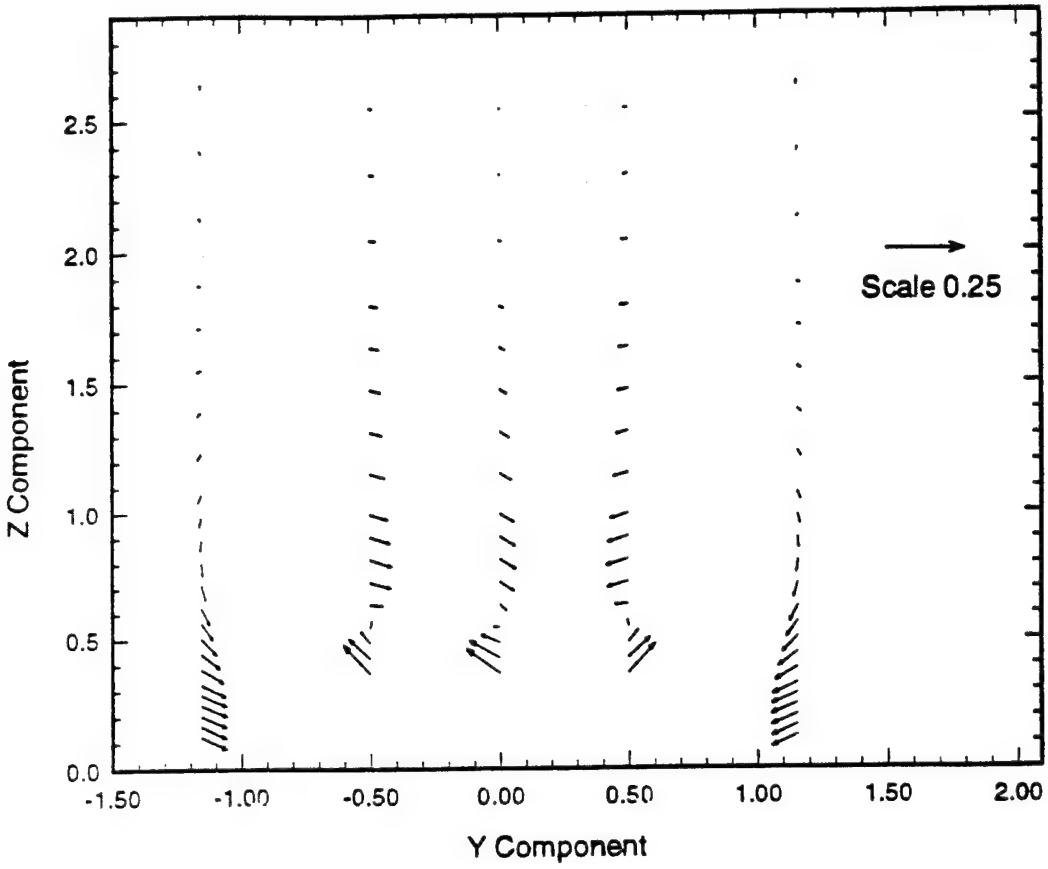

Figure 28. Cone Probe velocity vector plots at the cavity's leading edge for Mach number of 0.7 and 0.10 lbm/s mass injection using plate 4.

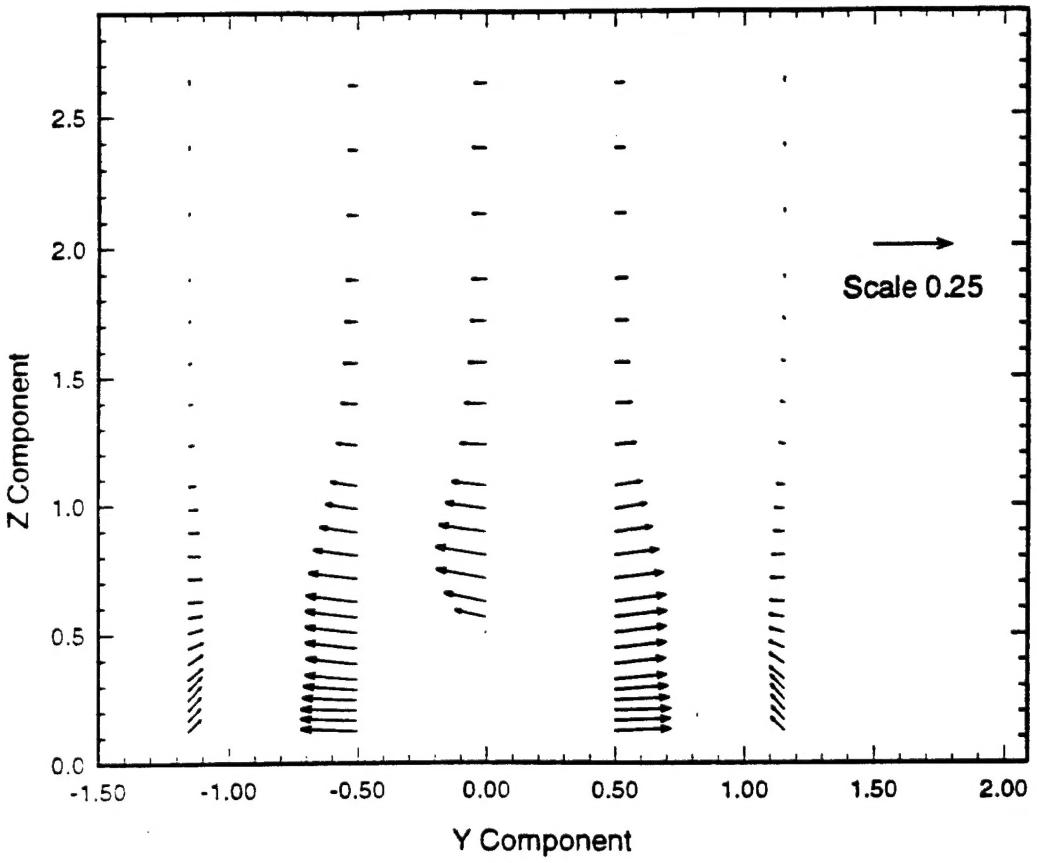

Figure 29. Cone Probe velocity vector plots at the cavity's trailing edge for Mach number of 0.7 and 0.10 lbm/s mass injection using plate 4.

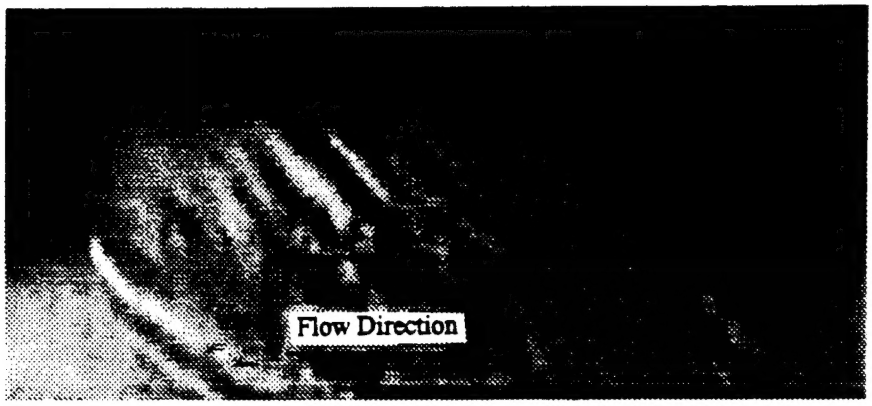

(a) Without Upstream Mass Injection

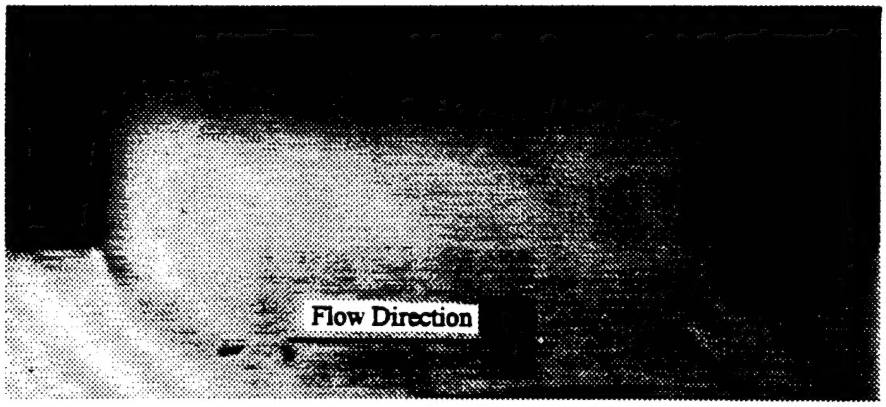

(b) With Upstream Mass Injection (4 gal/min)

Figure 30. Photographs of water table single cavity arrangement.

(a) Without Upstream Mass Injection

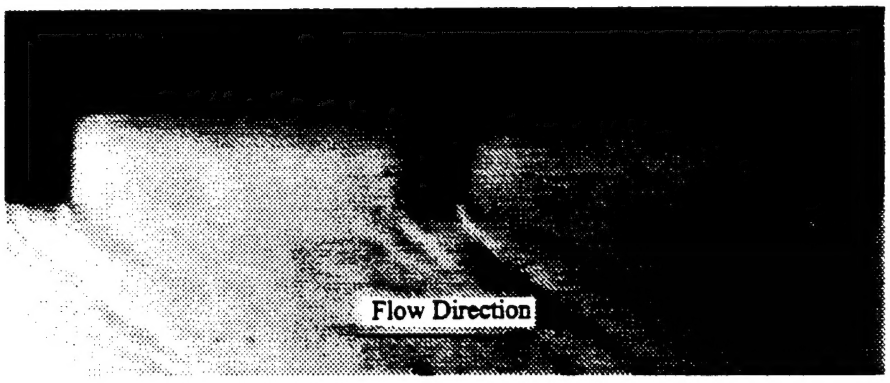

(b) With Upstream Mass Injection (4 gal/min)

Figure 31. Photographs of water table with double in-line cavity arrangement.

APPENDIX A

AND

APPENDIX B

ARE

BOUND

SEPARATELY